“CHANNELING THE GREEN DEAL FOR VENICE”
Action n. 2019-IT-TM-0096-S
CEF Connecting Europe Facility

HYDRODYNAMIC SIMULATIONS

Numerical modelling study of the vessel generated erosion along the Malamocco Marghera Channel – New Channel Configuration

Activity		**Phase 3**
Task		Numerical modelling study of the vessel generated erosion along the Malamocco Marghera Channel – New Channel Configuration
Authors		Grith Christoffersen Berry Elfrink, Project Manager Andrea Pedroncini, Project Manager
Dissemination Level		Restricted
Status		Issued for comments
Due date		
Document Date		17 May 2023
Version Number		1.1

Legal Disclaimer

CHANNELING THE GREEN DEAL FOR VENICE is co-funded by the European Commission, Connecting Europe Facility (CEF) programme under grant agreement No. INEA/CEF/TRAN/M2019/2112366 - Action No: 2019-IT-TM-0096-S. The information and views set out in this document are those of the author(s) and do not necessarily reflect the official opinion of the European Union.

LIST OF CONTENTS

APPENDICES

1 CONTENT

A series of comprehensive modelling activities was conducted to quantify the impact of maritime traffic on the Malamocco – Marghera Channel (abbreviated as MMC in the following) and surrounding areas. Possible solutions are identified aimed at minimizing the erosion processes that are now affecting the tidal flats surrounding the channel, thus achieving sustainable navigation conditions.

To match this ambitious goal, following Public Tender procedures, the Contract was awarded by Port of Venice to a Consortium led by DHI S.r.l. and formed by DHI A/S, Force Technology, HS Marine S.r.l., Cetena S.p.A. and Around Water di Andrea Zamariolo Ph.D. Geol.

The present document follows up on the study of the present day MMC-configuration reported in (DHI A/S 2022, [1]) by investigating the influence of reduced vessel speed, updated channel layout and reconstruction of salt marsh islands on the erosion along the MMC and surrounding areas.

Section 2 focuses on the changes made to the models during the incorporation of the new layout.

Section 3provides analyses and discussions of model results considering:

- the existing channel layout with reduced navigation speed (known as Mitigation Scenario a, abbreviated as MS-a in the following);
- the modified channel and surrounding areas layout with reduced navigation speed (known as Mitigation Scenario b, abbreviated as MS-b in the following).

Section 3 provides a conclusion summary.

With reference to the "*Capitolato Tecnico*" the present document includes the following deliverable:

21. *Relazione tecnica dei modelli di navigazione finalizzati alla validazione delle soluzioni progettuali e dei modelli idrodinamici finalizzati alla validazione delle soluzioni progettuali.*

2 PRODUCTION MODEL CHANGES DUE TO MITIGATION MEASURES

The present chapter outlines the changes made to the hydrodynamic and sediment transport model as a result of the selected measures for mitigating the erosion of the MMC tidal flats. For a detailed description of the model, the reader is referred to (DHI A/S 2022, [1]). An overview of the model domain extent is given in Figure 2.1.

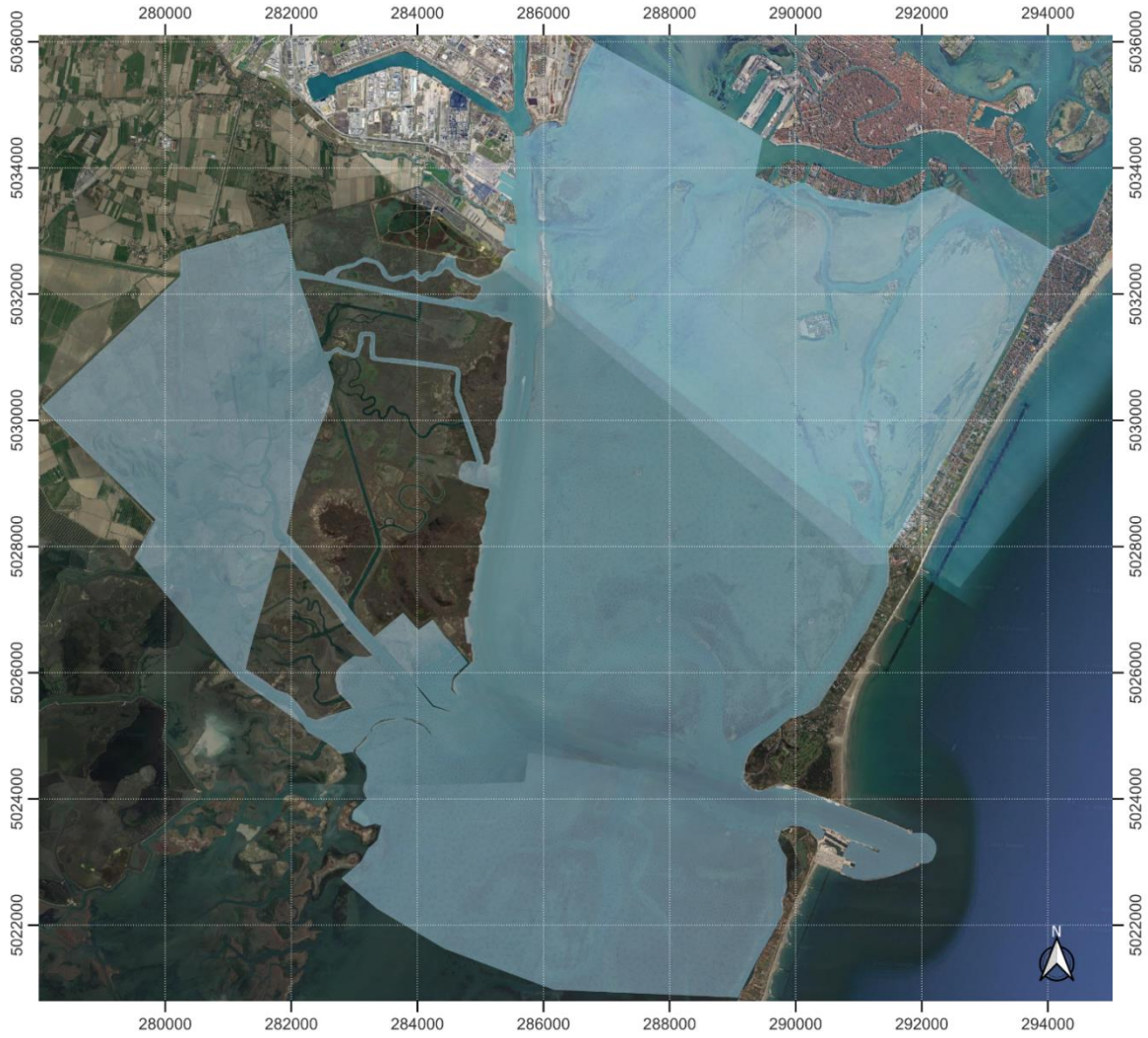

Figure 2.1. Extent of model domain for displacement wave modelling.

To model the erosive effect from the traffic in the MMC, the model considers a single vessel approach i.e., 6 representative vessel types have been identified, representative vessel geometries have been

selected for each type, a passage of a single representative vessel has been modelled and the erosion established. This result is then scaled accounting for the occurrence frequency of the vessel type. Consecutive passages have not been modelled. Vessel convoys make it difficult to establish the representative traffic (and quantify the erosion) as they provide several degrees of freedom e.g., the number of vessels in convoy, vessel types in convoy and time between vessels. Based on the PoV database 75%/25% of the passages take place with more/less than 10 minutes separation and the average separation time is about 20 minutes. Most of the suspended sediment (sand and silt fraction) settles after ~5-10 minutes (based on calibration results provided by Scarpa et al 2019). Hence generally most passages occur with sufficient separation time for the sandy and silty sediment to have settled and as such the single vessel approach is not an unreasonable assumption when it comes to assessing the erosion though the initial concentration encountered by a consecutive vessel may be higher than that encountered by a single passage.

2.1 Changes to model bathymetry and computational mesh

In Figure 2.2 an overview of the structural changes along the channel is shown. The new design contains:

- 8 new saltmarsh islands along the east side of the channel.
    - The polygons indicate the non-erodible part of the saltmarsh islands which will have a level of +0.8 m MSL.
- An extension of Isola delle Tresse in the Fusina area.
- Restoration of the existing reclamation area west of the channel, which moves the shoreline closer to the channel.
- Lowering of some existing structures to a level of -1.2 m MSL.
    - This change applies to the long breakwater marked by the dotted line as well as the small breakwater northwest of it.
    - In the model these structures are implemented as sub-grid structures, meaning that they are not resolved directly in the mesh. However, their main features and effects on the flow are resolved.

It should be noted that the extension of Isola delle Tresse and the restoration of the existing reclamation area west of the channel are included in the tested layout but they are not part of the mitigation measures studied within the present work, since the drawings have been made available by the Port Authority, derived from third parties projects / plans.

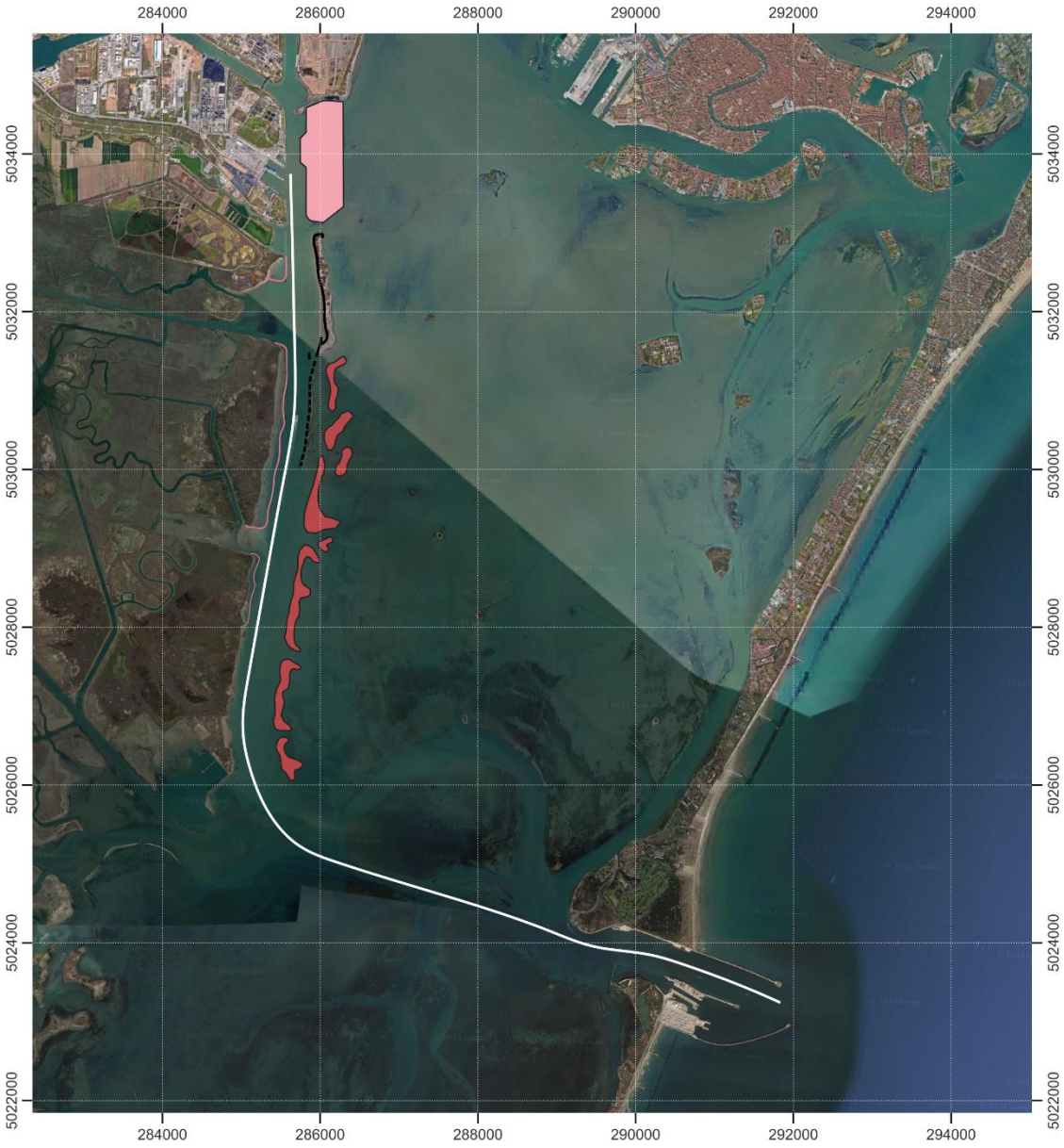

Figure 2.2 Overview of structural features in the new channel layout.

Coloured polygons indicate the implemented structures. The white line indicates the vessel trajectory.

Additionally, the new channel layout contains local widening and smoothing of the channel, see Figure 2.3. Note that the original vessel trajectory has been maintained. This has the consequence that the vessel is not located at the channel centre-line north of the Fusina bend. The alignment of the channel mesh with the vessel trajectory is mainly of importance for the numerical stability of the

model. As long as the mesh resolution is high enough to resolve the changes in the bathymetry, the evolution of the displacement waves will still be well represented by the model. Of course, the distance to the channel bank has an influence on the draw down level magnitude along the banks, but in reality, the vessel track is uncertain as it will vary from vessel to vessel depending on size, hydrodynamic - and traffic conditions at the time of passage. Hence the model results will in either case represent a simplified reality which requires some care during interpretation of the results.

An overview of the updated model bathymetry and computational mesh is shown in Figure 2.4. The thin black lines in the view of the bathymetry indicate a few selected contours: -1, -3 and -10 m MSL. The thick black lines indicate implemented structures, and the pink lines indicate three extraction lines numbered 1 to 3 starting from north.

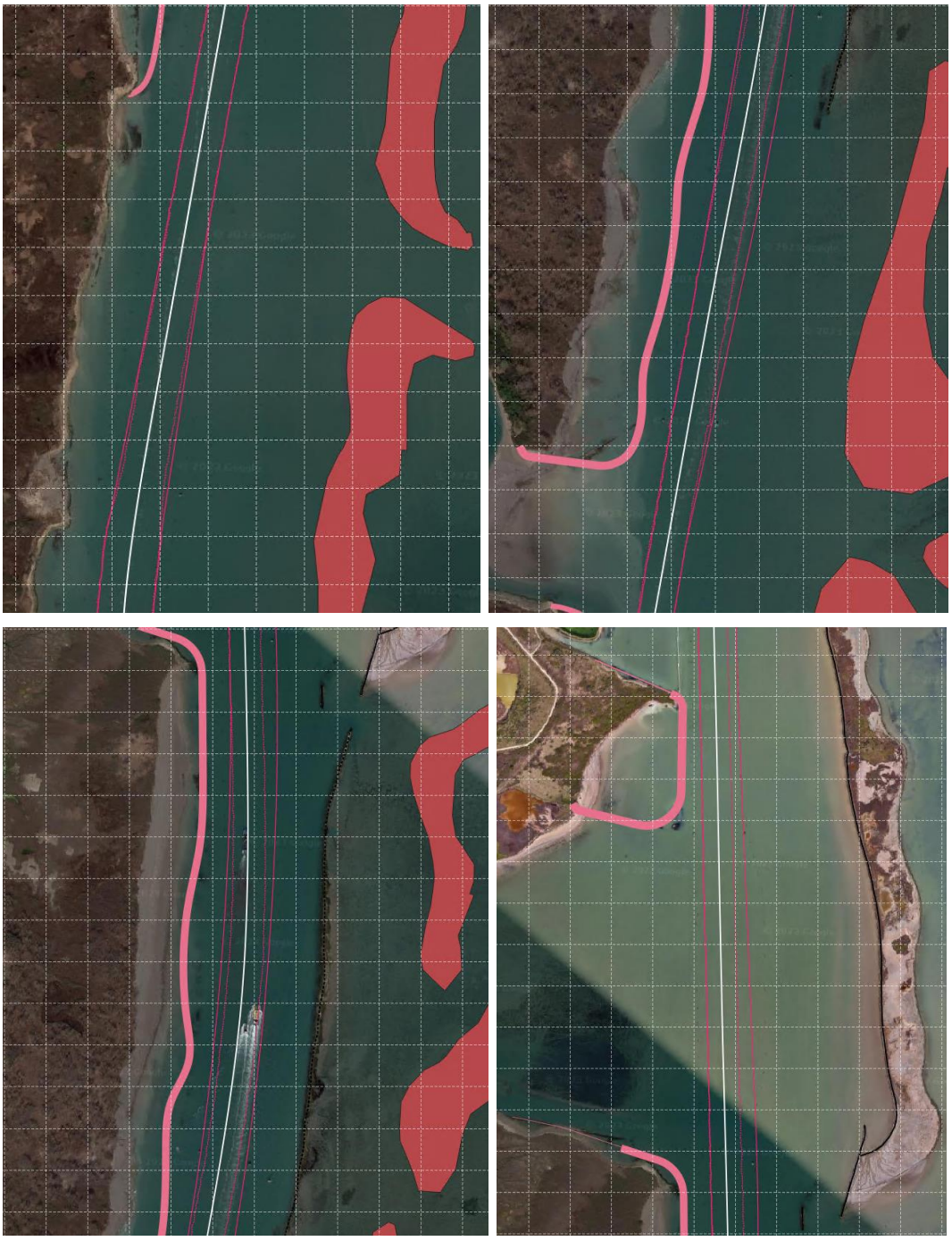

Figure 2.3 Smoothing and widening of channel.

White/Pink line show vessel trajectory/-10 m contour respectively. The inner-most contour indicates the original channel layout.

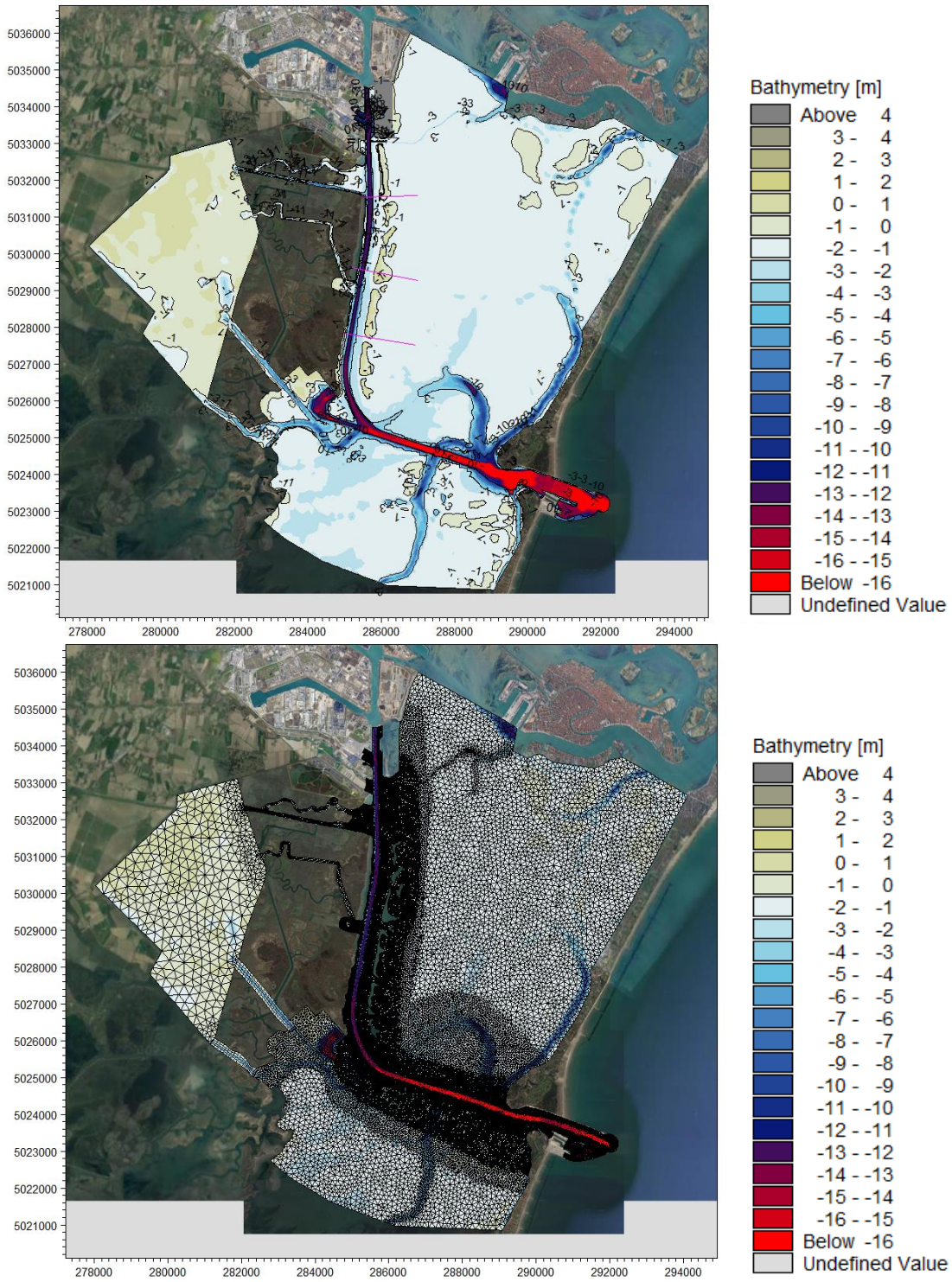

Figure 2.4. Full overview of model bathymetry (top) and computational mesh (bottom).

The computational mesh contains 783,412 elements. Most of which are used to resolve the MMC itself. This channel is resolved by 2x2 m quadrilateral elements over a cross sectional width of about 120 m. This very high resolution is required to provide a good representation of the moving vessel inside the channel. Moving away from the MMC, the computational mesh expands into triangular elements with 5 m resolution and then to about 10 m resolution. In the far field e.g., the central part of the lagoon, the resolution is about 150 m.

The vertical resolution of the domain consists of five equidistant sigma-layers, meaning that the water column consists of five vertical layers everywhere. In an area of 5 m water depth each layer will have a thickness of 1 m whereas in an area of 10 m water depth the layers will be 2 m thick. As such the layer thickness varies across the domain.

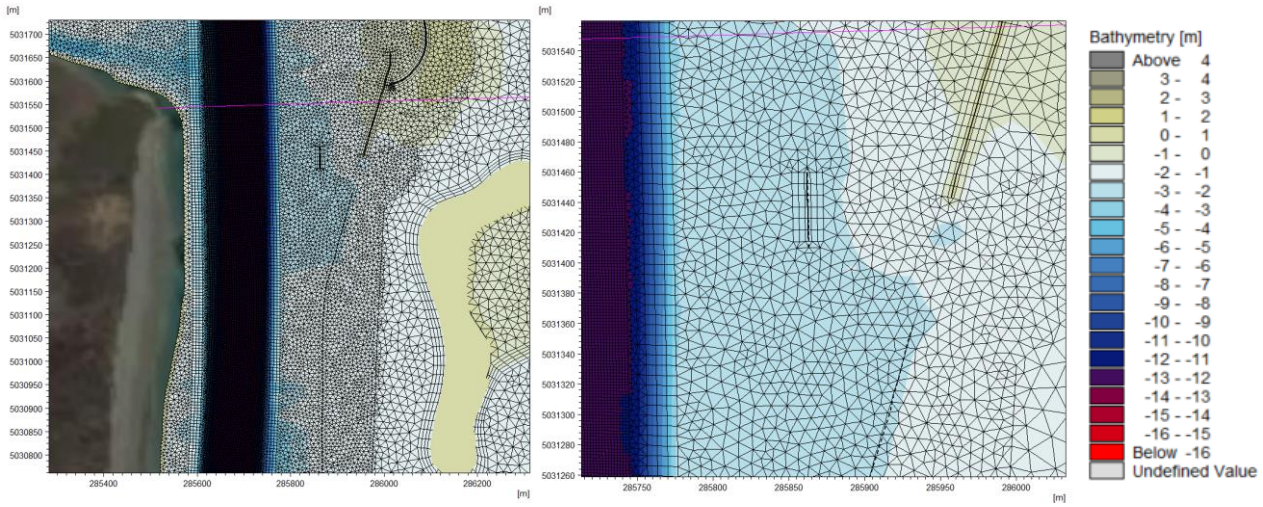

Figure 2.5. Zoomed view of computational mesh details.

2.2 Changes to vessel speed

One of the most important factors for mitigating the erosion of the MMC tidal flats is the vessel speed. The changes to the channel layout have enabled a reduction of the vessel navigation speed from 10 to 8 knots between the San Leonardo bend and Fusina. Extensive navigational simulations have shown that this reduced speed is safe for navigation, except under infrequent very intense wind conditions. In these conditions the 8 knots limit, for navigational safety reasons, will not apply.

Comparison between the original (constant navigation at 10 knots) and updated (navigation at 10 to 8 knots) speed profile for an in- and out-bound vessel passage is given in Figure 2.6 and Figure 2.7 respectively. The updated speed profile contains a linear change in navigational speed through the San Leonardo bend.

Considering that the changes to the bathymetry are minor and also relatively symmetric i.e., the centerline of the channel remains similar to existing conditions in most places, it has therefore been chosen to maintain the original navigational track for the updated model simulations. In some areas the turns have become somewhat smoother, but these effects are mainly important for navigational safety rather than the formation of the displacement waves.

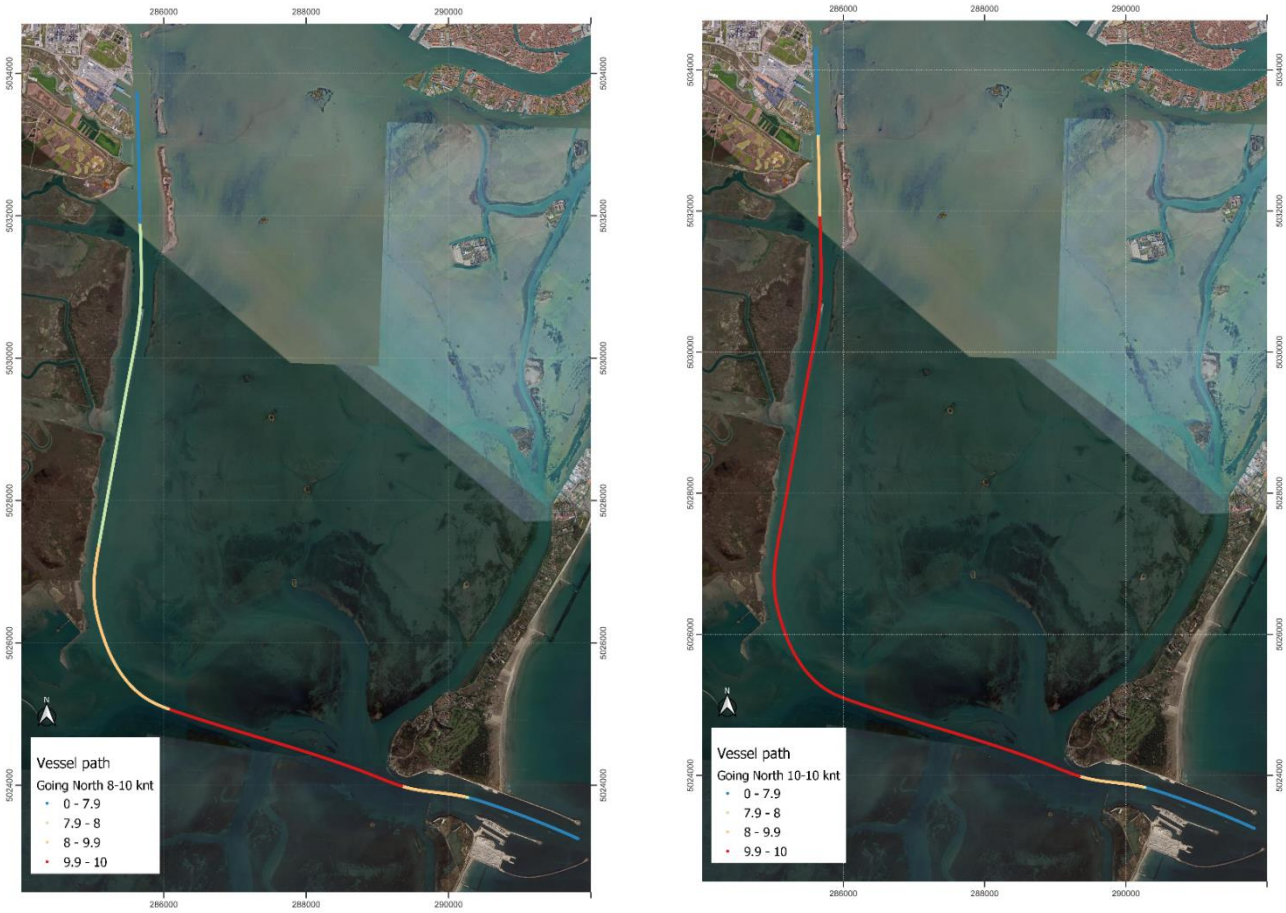

Figure 2.6. Production vessel track for in-bound passages. (Left) 10 to 8 knots and (Right) 10 knots.

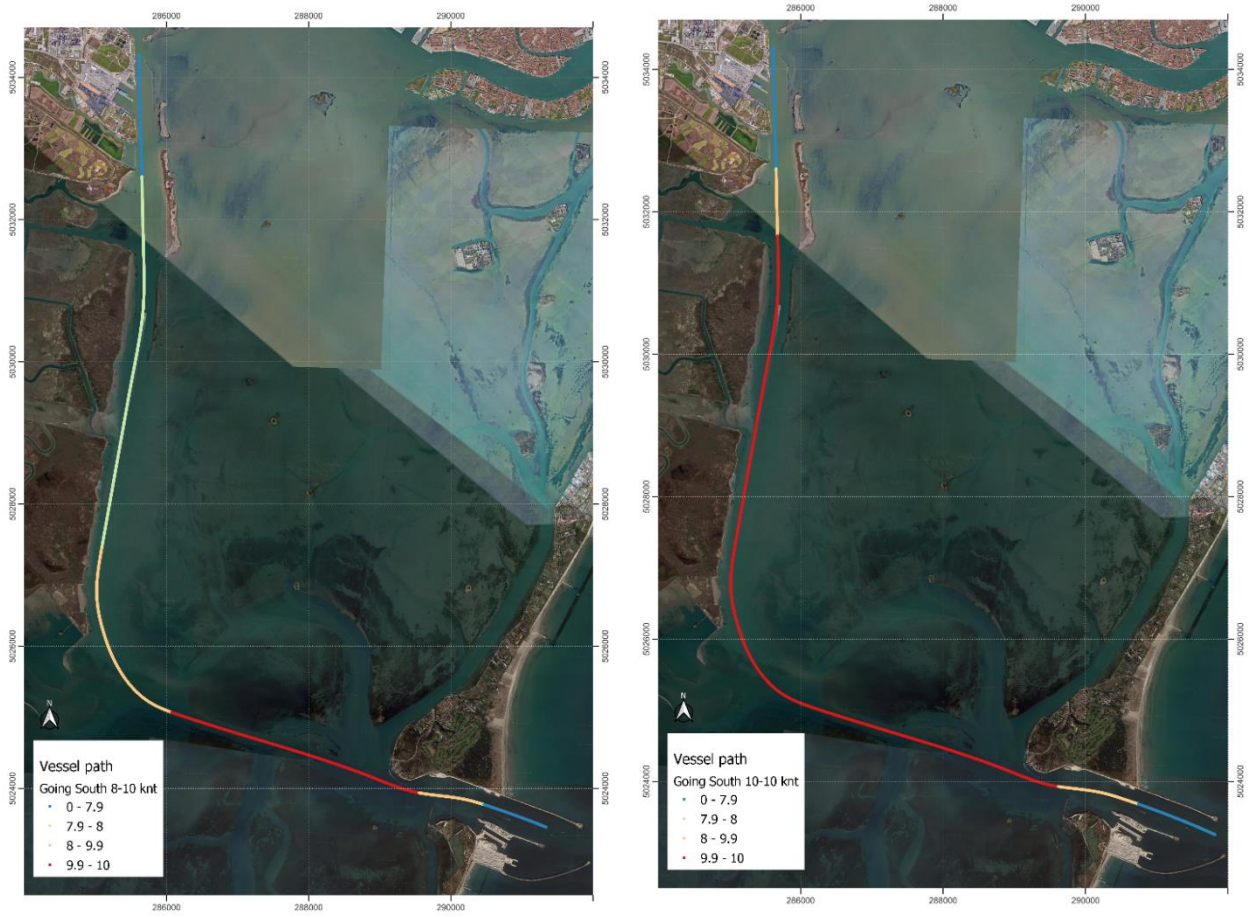

Figure 2.7. Production vessel track for out-bound passages. (Left) 8 to 10 knots and (Right) 10 knots.

2.3 Changes to sediment transport model

The original input files of the sediment transport model have been interpolated to the new computational grid ensuring that any values assigned to the originally somewhat narrower channel covers the re-designed wider channel. Hence generally no significant changes have been made to the sediment transport model.

The implemented salt marsh islands contain an erodible part facing east into the lagoon. The bed shear stress limits of these specific areas have been set similar to the original salt marsh areas i.e., 1.8 Pa for erosion and 0.7 Pa for deposition, see Figure 2.8.

Figure 2.8 Updated map of critical bed shear stress for erosion of top sediment layer.

3 PRODUCTION MODELLING OF MITIGATION MEASURES

In the present section the results of the production modelling considering the updated vessel speed profile (shown above in Figure 2.6 - Figure 2.7) and using the updated layout, will be presented. The presented results from modelling of displacement waves consist of the following tasks:

1. Baseline modelling (presented in detail in (DHI A/S 2022, [1])
2. Mitigation modelling (present report)

The modelling seeks to illustrate the representative vessel traffic of the MMC by use of the vessels listed in Table 3-1 based on data provided by the Port of Venice (PoV).

Table 3-1. Vessel geometries from PoV Database.

Vessel Type	Name	Length Percentile	Abbr. Name	Length (m)	Breadth (m)
Container vessel	Atlantic Silver	50	Con. S	175.1	27.9
Container vessel	Lavaux	75	Con. L	199.6	29.8
Tanker vessel	Minstrel	50	Tan. S	161.1	23.0
Tanker vessel	AS Pamira	75	Tan. L	179.9	32.2
Bulk carrier	MSC Asli	50	Bul. S	175.6	23.1
Bulk carrier	Valsesia	75	Bul. L	190.0	28.5
General cargo	Syn Zaura	50	Gen.	109.7	17.8
Ro-Ro	Loyal	50	Ro-Ro	200.9	26.5
Cruise vessel	-	-	Cru. S	230	-
Cruise vessel	-	-	Cru. L	300	-

Based on the PoV Database the occurrence of passages for each vessel category were established:

1. Container vessels, 27.1% of events
2. Tanker vessels, 20.5% of events
3. Bulk carriers, 15.5% of events
4. General cargo vessels, 15.3% of events
5. Ro-Ro vessels, 14.6% of events
6. Cruise vessels

The five main categories make up 93% of the events in the PoV Database and therefore practically represent the entire traffic in the MMC.

As agreed with PoV, the cruise vessels should be included with one passage per week from 1st April to 1st November (30 weeks), hence 120 events (in-bound + out-bound). Relative to the total number of events in the PoV Database this is about ~2% of the time.

Summary of baseline procedure

During the baseline modelling, all selected vessels were simulated considering in-bound and out-bound passage (towards Fusina/Malamocco respectively). The navigation speed in all simulations was 10 knots and the ambient water level was set to zero m MSL. Each model run contained an acceleration/deceleration phase to/from 10 knots at the beginning and end of the track. The acceleration/deceleration of the vessel was about 12/20 minutes respectively to avoid numerical shock waves from forming in the model.

The accumulated effect on the erosion from the traffic over 1 year was calculated by considering the weighted contribution of each selected vessel category as shown in Table 3-2.

Table 3-2. Number of in- and out-bound passages per year per vessel type of representative traffic.

Abbr. Name	Length percentile	Total no. per year	Weight	No. in-bound	No. out-bound
Con. S	50	1286	0.75	482	482
Con. L	75		0.25	161	161
Tan. S	50	974	0.75	365	365
Tan. L	75		0.25	122	122
Bul. S	50	734	0.75	275	275
Bul. L	75		0.25	92	92
Gen.	50	734	1	367	367
Ro-Ro	50	691	1	346	346
Cru. S	-	60	1	30	30
Cru. L	-	60	1	30	30

A detailed run through of the results of the small and most frequent container vessel (Con-S) was given. Then tabularized hydrodynamic results of the simulations were presented and discussed and finally the weighted accumulated bed changes were analysed.

Procedure for analyses of effect of mitigation measures

A series of additional model simulations will be carried out to investigate the influence from the selected Mitigation Scenarios (MS):

a) Effect from reduction of speed.
   - Original channel layout with 8 knot navigational speed between Fusina and the San Leonardo bend.
   - Two vessels: Con-S (most frequent) and Tan-L (causes most erosion of the MMC tidal flats).

b) Effect of modified layout and reduced speed.
   - Updated channel layout with 8 knot navigational speed between Fusina and the San Leonardo bend.
   - All vessels.

Similar to the baseline simulations, tabularized results and bar charts of minimum water level (maximum draw down level) will be provided, compared and discussed relative to the baseline results considering Mitigation Scenario a and b (MS-a and MS-b in the following). The erosion will be calculated and discussed relative to baseline conditions considering single passages for MS-a and MS-b and accumulated over a full year considering MS-b.

3.1 Overview of evaluation locations

The present section provides an overview of the extraction locations used in the assessment of the model results.

3.1.1 Extraction lines

The tabularized hydrodynamic results consider values extracted along the three lines indicated in Figure 3.1. Considering the original channel design, Line-2 and Line-3 were not restricted by any structures and thus provided information on how the draw down evolved during its propagation into the lagoon. The results were extracted at the points indicated in Table 3-3 and Table 3-4 below, see also Figure 3.2 for bathymetric details along the lines.

But with the new layout, Line-2 and Line-3 are now confined by the new salt marsh islands. Therefore, direct comparisons with the previous results east of the channel will be made considering the extraction point at the original channel margin and 200 m from the original channel centre only.

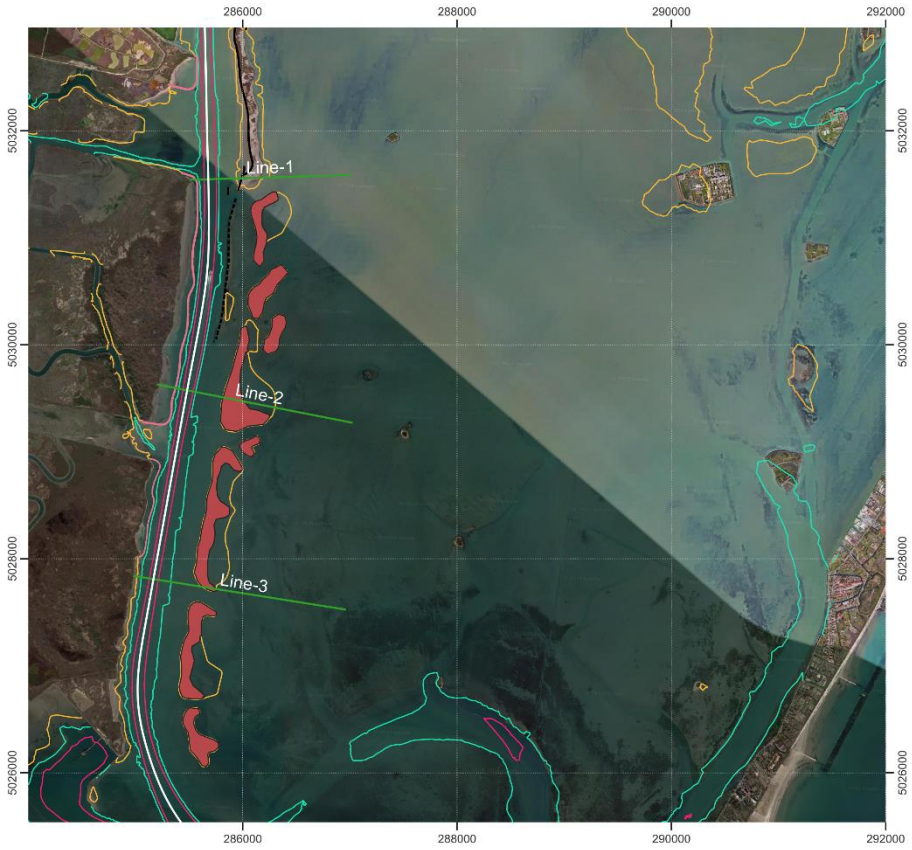

Figure 3.1 Illustration of the location of the three output lines.
Green lines mark the output lines.

Table 3-3. Bathymetric depths of line extraction points east of the channel considering the original/new layout respectively.

Depth (m MSL)	Margin	200 m	400 m	600 m	800 m	1000 m	1200 m	1400 m
Line-1	4.4 / 10.4	2.1 / 2.0	- / 0.1	1.5 / 1.3	1.4 / 1.5	1.5 / 1.4	1.6 / 1.6	1.6 /1.6
Line-2	5.9 / 8.0	2.0 / -2.0	1.6 / -	1.5 / -	1.5 / 0.2	1.4 / 1.4	1.6 / 1.6	1.7 / 1.7
Line-3	5.3 / 5.4	2.5 / 2.5	1.9 / 1.8	1.7 / 1.4	1.7 / 1.7	1.7 / 1.7	1.7 / 1.7	1.8 / 1.8

Table 3-4. Bathymetric depths of line extraction points west of the channel considering the original/new layout.

Depth (m MSL)	Margin	75 m	100 m	125 m	150 m
Line-1	5.8 / 5.3	3.5 / 3.8	1.3 / 1.8	0.6 / -	- / -
Line-2	5.9 / 5.2	4.5 / 4.0	3.1 / 2.4	2.9 / -	2.2 / -
Line-3	5.8 / 5.5	5.8 / 5.5	2.6 / 3.7	1.3 / 2.5	0.7 / 1.3

Based on Figure 3.2 the original channel cross section is wider at Line-3 than at Line-1 and Line-2. Hence smaller draw down magnitudes should be expected at Line-3 than at Line-1 and Line-2.

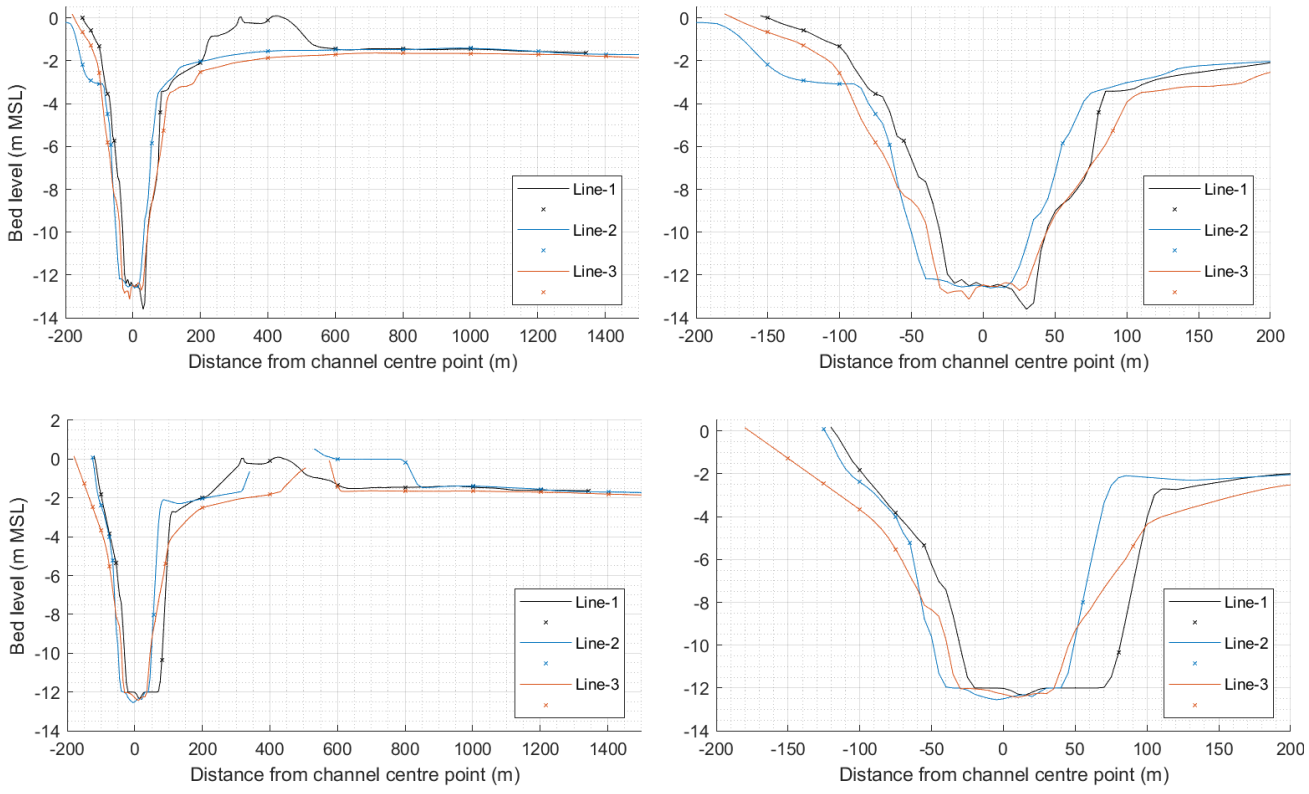

Figure 3.2. Visualization of bathymetry along extraction lines considering original (top) and new (bottom) layout.

Left: entire cross section, Right: zoom of the channel area.

With the new layout, the channel cross section with a water depth greater than 10 m MSL has widened by about:

- Line-1: 40 – 50 m, slopes towards western reclamation area and lagoon have become steeper.
    - All in all, a less restrictive cross section for the draw-down wave.
- Line-2: 20 m, slopes towards western reclamation area and lagoon have become steeper.
    - All in all, a somewhat more restrictive cross section for the draw down wave.
- Line-3: 10 m, slopes towards western reclamation area and lagoon have become more linear and somewhat smoother.
    - All in all, a less restrictive cross section for the draw down wave.

3.1.2 Erosion polygon

To easily compare the effect of the mitigation measures on the erosion from the displacement waves, the eroded volume (i.e., the eroded volume adhering from the sum of negative bed changes) in the polygon shown in Figure 3.3 will be calculated for each vessel and each scenario (including the baseline). The polygon covers part of the existing channel slopes from around -5/-3 m MSL and onto the tidal flats east of the channel encapsulating the 0.7 Pa bed shear stress extent of the baseline conditions.

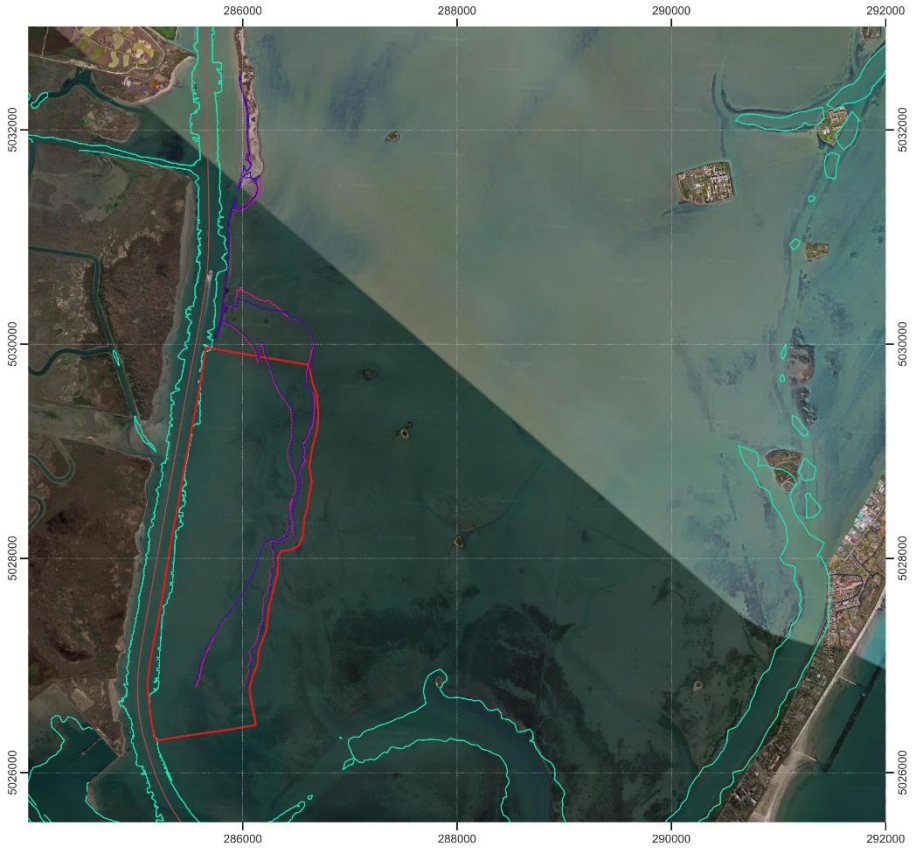

Figure 3.3 Map of erosion polygon.

(Solid red frame) Erosion polygon. (Purple/Pink contours) 0.7 Pa contour of maximum modelled bed shear stress during existing conditions from Cru-L/Bul-L respectively. (Cyan lines) -3 m MSL contour.

3.2 MS-a: Reduced navigation speed

3.2.1 Modelled draw down levels

Figure 3.4 to Figure 3.6 present bar charts of the minimum water level comparing baseline conditions to MS-a conditions. The bar charts consider the tidal flats on the east side of the channel at Line 1 to 3 respectively and illustrate how the draw down level magnitude varies:

- between the vessels (Con-S and Tan-L)
- between in-/out-bound directions
- how it decreases with distance from the channel at Line-2 and Line-3.

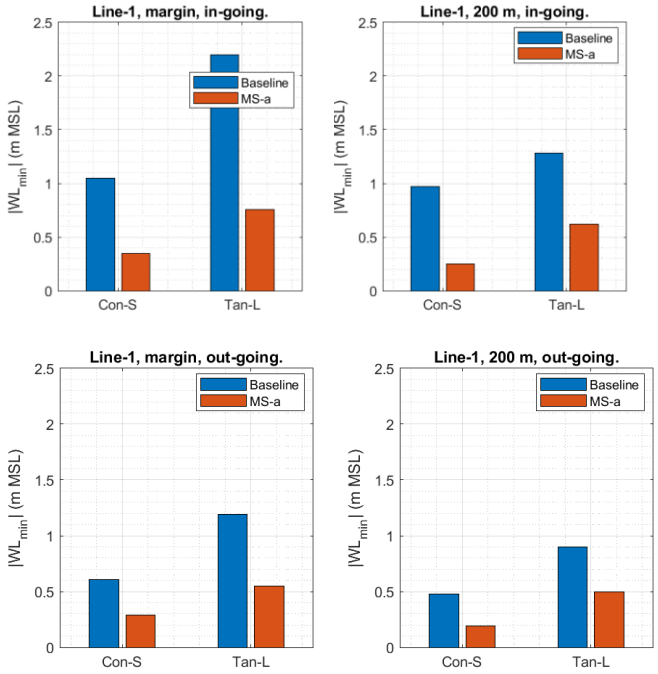

Figure 3.4. Bar chart of minimum water level at Line-1 during in- and out-bound passages for MS-a.

Note that in Appendix A tables of the draw down level magnitude east and west of the channel are provided considering MS-a conditions.

The decrease in navigation speed is seen to have a very large influence on the draw down level magnitude e.g., for Con-S the draw down level magnitude has decreased by about 55% to 74% along the points of the extraction lines compared to baseline conditions. Considering Tan-L the decrease in draw down level magnitude is in the range 47% to 68%.

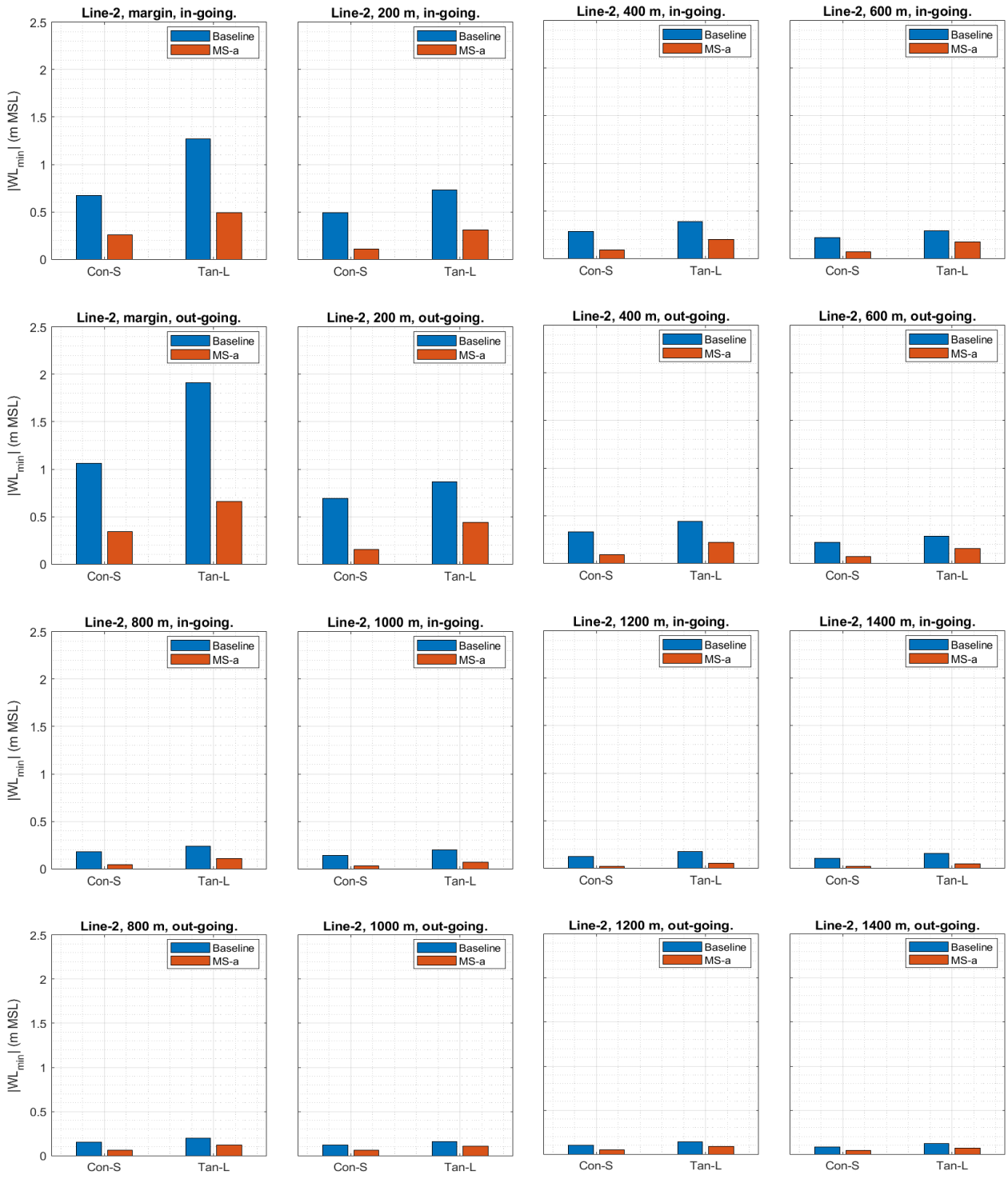

Figure 3.5 Bar chart of min water level at Line-2 during in- and out-bound passages for MS-a.

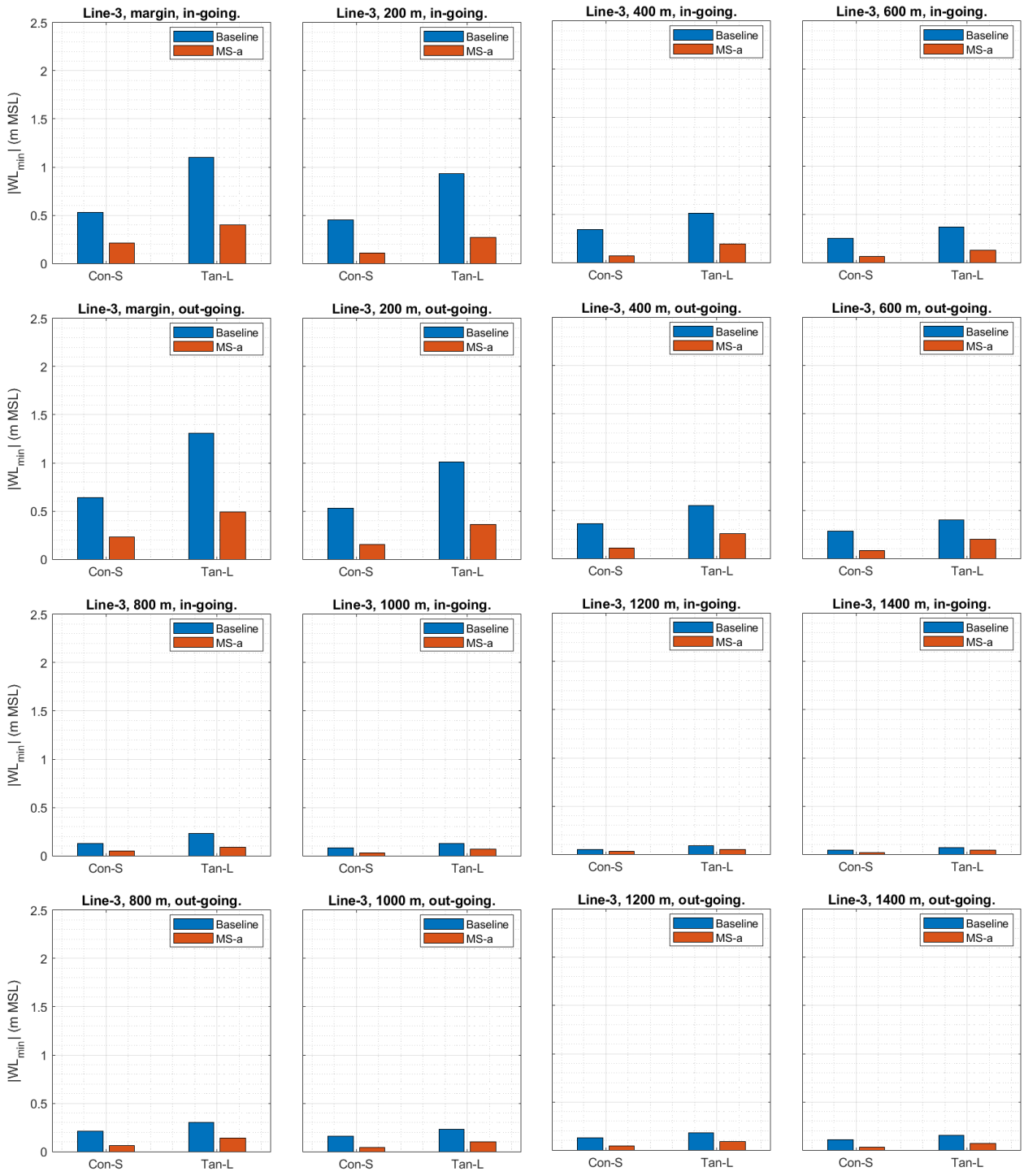

Figure 3.6 Bar chart of min water level at Line-3 during in- and out-bound passages for MS-a.

3.2.2 Modelled erosion and bed shear stress

In Table 3-5 the eroded volume in the erosion polygon, see Figure 3.3, is summarized for MS-a and baseline conditions. The table statistics are given for Con-S and Tan-L only, below an explanation of the table content is provided.

- Single Passage: Accumulated effect of in- and out-bound passage of one vessel.
  - In the first two columns the relative distribution of eroded volume per single vessel passage is considered. This makes it possible to evaluate the relative erosion potential of each vessel as follows for each scenario:

$$\frac{V_i^-}{\sum_{i=1}^{N_{vessels}} V_i^-} \cdot 100\% \quad , \quad i = 1{:}\,N_{vessels}$$

  - In the third column, the erosion volume change relative to baseline conditions is evaluated to illustrate the effect of the mitigation measure.

$$\frac{V_{i,MS-a}^- - V_{i,baseline}^-}{V_{i,baseline}^-} \cdot 100\% \quad , \quad i = 1{:}\,N_{vessels}$$

- Accumulated 1 year: Accumulated effect of in- and out-bound passages per vessel for 1 year assuming:
  - the number of occurrences listed in Table 3-2.
  - that the 8 knots navigational speed limit is valid 95% of the time.

Looking at the baseline conditions it is seen that Tan-L is responsible for 86% of the erosion in the polygon considering a single passage and 67% considering a full year – despite the fact that the assumed occurrence frequency of Tan-L is about 75% lower than that of Con-S. This illustrates that reducing the navigation speed of the largest vessels will have significant influence on the erosion.

Looking at the accumulated effect of Con-S and Tan-L over 1 year with 8 knots speed limit, the modelled eroded volume in the polygon has decreased by about 21,000 m^3 (about 85%) compared to existing conditions with 10 knots speed limit. Hence a significant reduction in erosion magnitude along the eastern banks of the channel is achieved by reducing the navigational speed by 20%.

The reduction in speed has caused the relative erosion distribution between the two vessels to change by about 10%-points: Con-S navigating at 8 knots is responsible for about 23% of the erosion as opposed to 33% with the 10 knots speed limit – a decrease in relative importance. Whereas for Tan-L the opposite is seen i.e., an increase in relative importance from 67% to 77%.

Table 3-5 Eroded volume in polygon considering MS-a.

Relative distribution indicated for single passage (in- + out-bound) and across full year applying the number of occurrences from Table 3-2. Change is calculated as scenario relative to baseline. Bottom row contains the total volume magnitude of each column.

	Single Passage			Accumulated 1 year		
	Baseline (%)	MS-a (%)	Change (%)	Baseline (%)	MS-a (%)	Change (%)
Con. S	14.0	<1	-100	33	22.5	-90
Con. L	-	-	-	-	-	-
Tan. S	-	-	-	-	-	-
Tan. L	86.0	100.0	-92.8	67	77.5	-83
Bul. S	-	-	-	-	-	-
Bul. L	-	-	-	-	-	-
Gen.	-	-	-	-	-	-
Ro-Ro	-	-	-	-	-	-
Cru. S	-	-	-	-	-	-
Cru. L	-	-	-	-	-	-
Total (m^3)	~120	~7.5	~ -112	~24,700	~3,600	~ -21,100

To illustrate the importance of the vessel displacement stencil for the erosion magnitude, the relative contribution for a single passage is plotted in Figure 3.7 considering baseline channel conditions. Note that the plot is for a single passage i.e., it does not account for occurrence frequency, but simply illustrates the erosion impact potential for each vessel. The figure indicates that displacement stencils:

- smaller than about 20,000 m^3 have a quite limited erosion potential.
- above ~25,000 m^3 but below ~35,000 m^3 have a 'moderate' erosion potential.
- above ~35,000 m^3 have a large erosion potential.

It is thus crucial for the lagoon sediment budget that compliance with the 8 knots navigational speed limit is prioritized and ensured considering frequently occurring vessels with moderate erosion potential (more than about 400 incidents, sum of in- + out-bound, per year and displacement stencils larger than about 25,000 m^3) and for large vessels with high erosion potential (displacement stencils larger than about 35,000 m^3) – especially if the occurrence frequency of the large vessels increases.

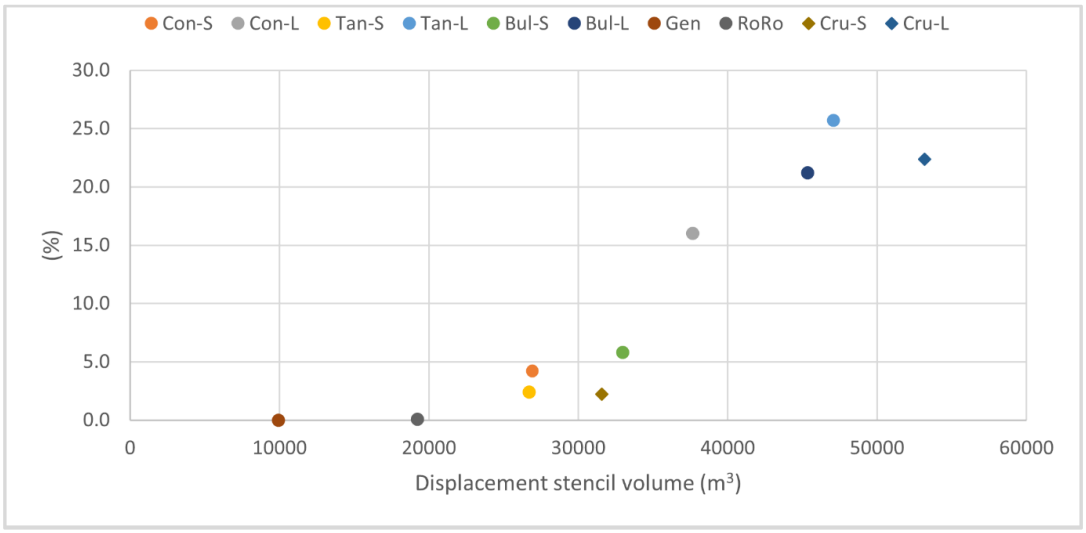

Figure 3.7 Relative erosion magnitude from single passages (in+out) of baseline channel conditions and vessel speed of 10 knots.

Of course, the two chosen vessels do not cover the full model traffic. But they do represent about 40% of the erosion in the polygon from the full modelled traffic and as such they give a quite good indication of the full erosion reduction potential from decreased vessel speed.

One aspect, which is important to keep in mind, is that these simulations have been made using the original computational mesh. This means that the eastern flats covered by the erosion polygon do not contain any structures. From the maps of the maximum modelled bed shear stress (Figure 3.8) it is clear, that the reduction in speed has a significant beneficial influence on the bed shear stress magnitude. It is however also clear that the bed shear stresses are larger in the area where existing structures align the existing channel. Special attention should be indeed focused on the proper placement of the new morphological structures (salt marshes) that will border the eastern side of the channel, to avoid possible erosion of the channel banks in case the effective dissipation area of the displacement waves would be reduced.

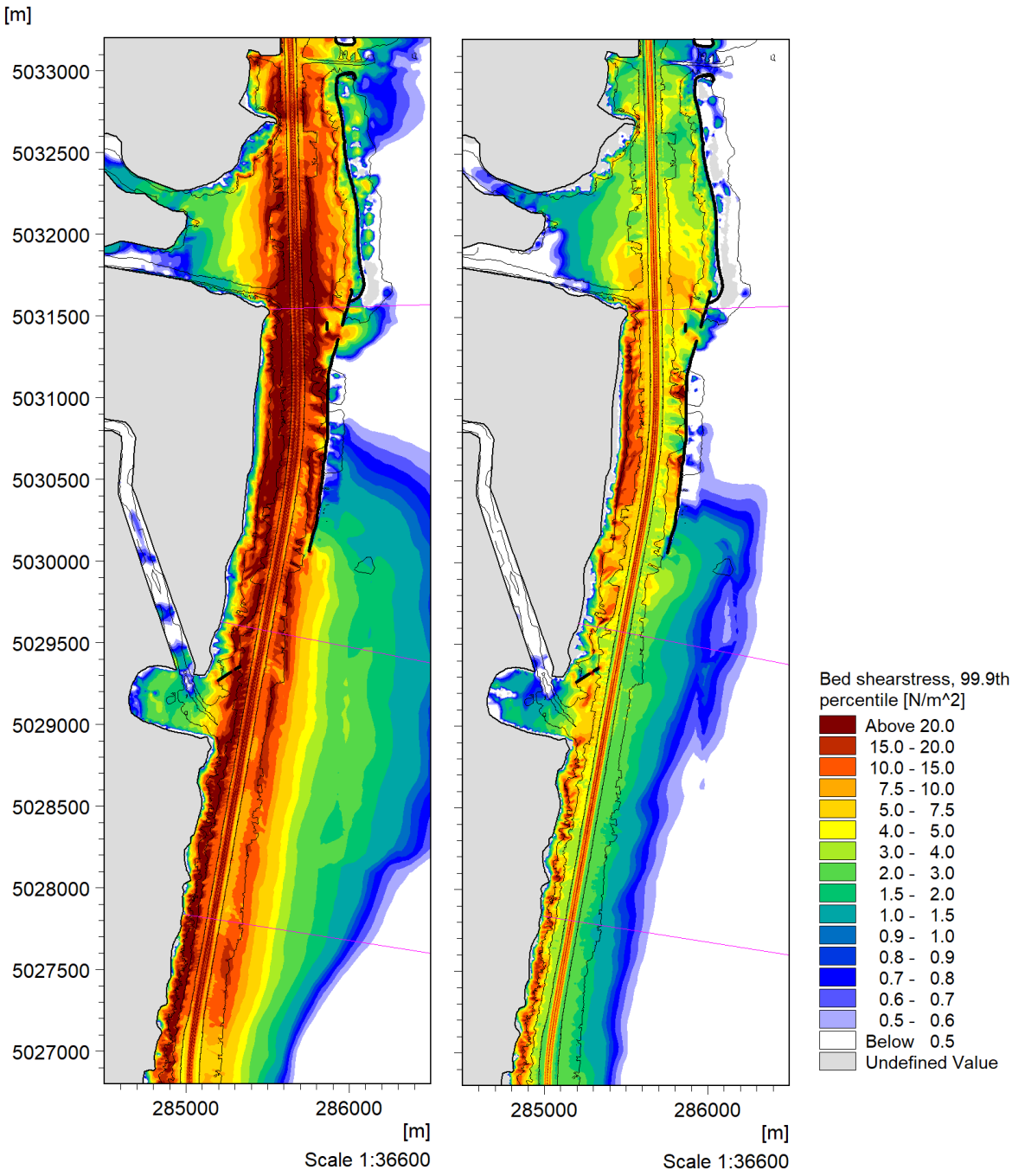

Figure 3.8 *Map of maximum bed shear stress during in-bound passage of Tan-L, MS-a.*

(Left) Existing channel, 10 knots. (Right) Existing channel, 8 knots. Extraction lines marked by pink lines, structures by thick solid black lines and -10, -3 and -1 m MSL contours by thin black lines.

3.3 MS-b: Reduced navigation speed and updated layout

3.3.1 Modelled draw down levels

Figure 3.9 to Figure 3.11 present bar charts of minimum water level comparing baseline conditions to MS-b conditions. The bar charts consider the tidal flats on the east side of the channel at Line 1 to 3 respectively and illustrate how the draw down level magnitude varies:

- between the vessels
- between in-/out-bound directions

Note that in Appendix B tables of the draw down level magnitude east and west of the channel are provided considering MS-b conditions and in Appendix C maps of the modelled suspended sediment concentration (SSC) is given. Note that the SSC results do not account for the effect of consecutive vessel passages.

From Section 3.2 it was concluded that the decrease in navigation speed already had a very large influence on the draw down level magnitude without any change to the channel layout. In the present section the combined effect of reduced speed and re-designed channel layout, combined with the reconstruction of salt marshes islands, is investigated.

At Line-1 (Figure 3.9), where the channel section with water depth larger than 10 m has been widened by about 40 – 50 m and the bend smoothed, the new channel design causes a further decrease in the draw down magnitude relative to MS-a conditions:

- East of channel:
    - Margin: 20% to 30% reduction in draw down level magnitude considering Con-S and Tan-L respectively relative to original layout with 8 knot speed.
    - 200 m from channel centre: 10% to 24% reduction in draw down level magnitude considering Con-S and Tan-L respectively relative to original layout with 8 knot speed.
- West of channel:
    - Margin: 2.5% to 1.4% reduction in draw down level magnitude considering Con-S and Tan-L respectively relative to original layout with 8 knot speed.
    - 75 m from channel centre: 3.2% to 11% reduction in draw down level magnitude considering Con-S and Tan-L respectively relative to original layout with 8 knot speed.

- 100 m from channel centre: 6.5% to 1% reduction in draw down level magnitude considering Con-S and Tan-L respectively relative to original layout with 8 knot speed.

The reduction (due to the redesigned channel) is generally smaller west of the channel at Line-1 than towards east. The reason for this is that the widening of the channel mainly happens on the east side of the channel here and that the western shoreline has been moved closer to the channel due to restoration of the western reclamation areas.

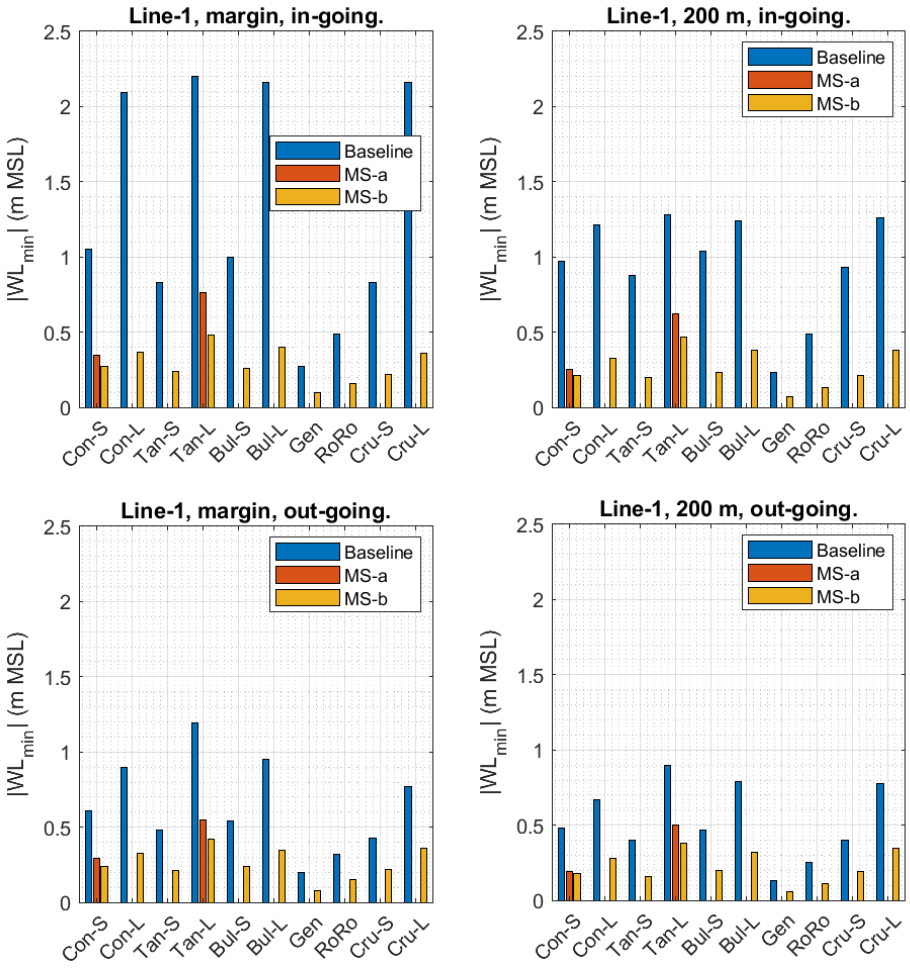

Figure 3.9. Line-1 minimum water level during in- and out-bound passages for MS-b.

At Line-2 (Figure 3.10), where the channel section with water depth larger than 10 m has been widened by about 30 m (mainly on the east side), the new layout causes an increase in the draw down magnitude relative to MS-a conditions (opposite to the further decrease seen at Line-1):

- East of channel:
    - Margin: 17% to 12% increase in draw down level magnitude considering Con-S and Tan-L respectively relative to original layout with 8 knot speed.
    - 200 m from channel centre: 80% to 37% increase in draw down level magnitude considering Con-S and Tan-L respectively relative to original layout with 8 knot speed.
- West of channel:
    - Margin: 29% to 47% increase in draw down level magnitude considering Con-S and Tan-L respectively relative to original layout with 8 knot speed.
    - 75 m from channel centre: 39% to 52% increase in draw down level magnitude considering Con-S and Tan-L respectively relative to original layout with 8 knot speed.
    - 100 m from channel centre: 78% to 91% increase in draw down level magnitude considering Con-S and Tan-L respectively relative to original layout with 8 knot speed.

However, MS-b conditions still represent a considerable reduction in drawdown magnitude when compared to baseline conditions. This is evident from the bar charts in Figure 3.10 and it also applies to the west side of the channel. In addition, it should be always taken into account that while the lowering by 2 knots of the vessel speed will have a significant influence on the navigation impact, in unfair weather conditions ships can accelerate in order to gain safe maneuvering speed. This means that in unfair weather conditions the navigation impact will not be negligible. Therefore, it is still required to maximize the channel safety in order to reduce the number of events when the speed limits could be exceeded for safety reasons. Moreover, structural optimization are still required at critical points where the existing channel is too narrow or additional structure narrowing the effective channel section are going to be restored (land reclamation south of Fusina) or built (new Isola delle Tresse).

The reason for the increase in draw down magnitude relative to MS-a conditions is related to two aspects which limits the spreading of the draw down wave:

- The western shoreline has been moved closer to the channel due to the restoration of the western reclamation area.
- The channel slopes have become slightly steeper compared to existing conditions.
    - This effect will likely decrease within a relatively short time frame (a couple of years) due to erosion of the channel slopes from the vessel traffic.

- The implemented salt marshes east of the channel slightly restrict the draw down wave from spreading into the lagoon east of the channel.

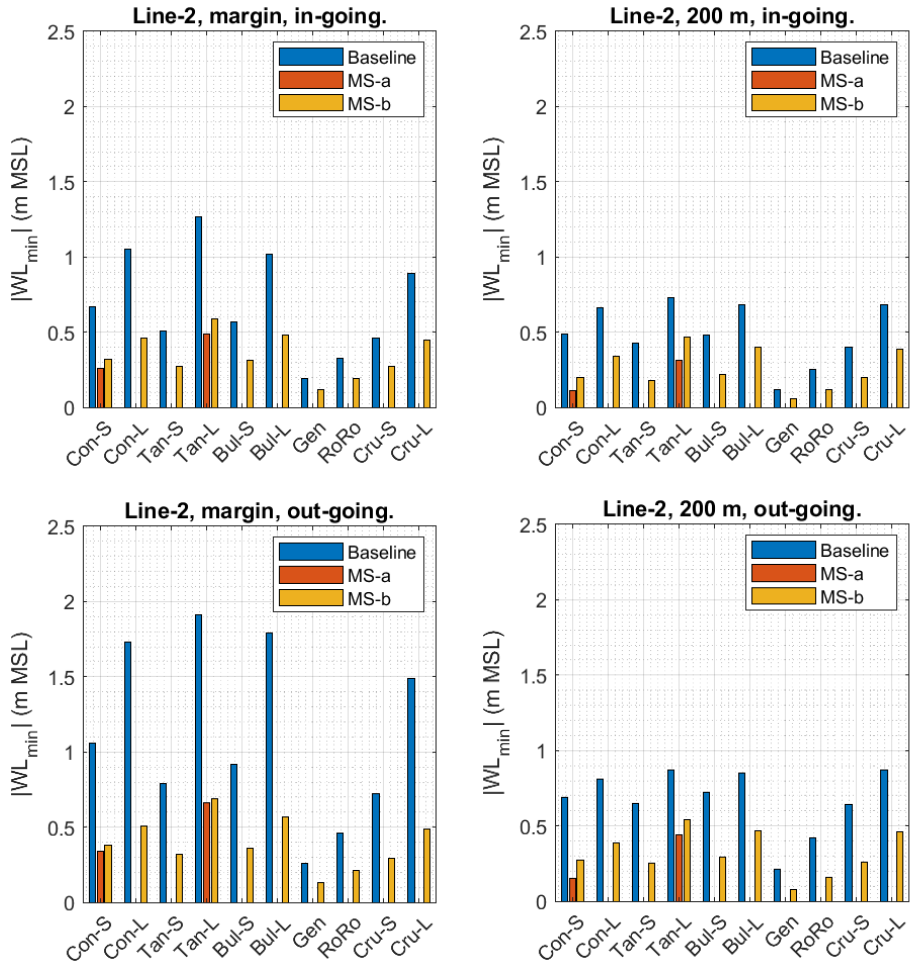

Figure 3.10 Line-2 minimum water level during in- and out-bound passages for MS-b.

At Line-3 (Figure 3.11), the channel cross section remains quite similar to existing conditions but east of the channel salt marsh islands have been implemented about 450 m from the channel. The new channel design causes a small increase in the draw down magnitude relative to MS-a conditions:

- East of channel:
  - Margin: 9% to 10% increase in draw down level magnitude considering Con-S and Tan-L respectively relative to original layout with 8 knot speed.

- 200 m from channel centre: 28% to 24% increase in draw down level magnitude considering Con-S and Tan-L respectively relative to original layout with 8 knot speed.

- West of channel:
  - Margin: 10% to 15% increase in draw down level magnitude considering Con-S and Tan-L respectively relative to original layout with 8 knot speed.
  - 75 m from channel centre: 10% to 15% increase in draw down level magnitude considering Con-S and Tan-L respectively relative to original layout with 8 knot speed.
  - 100 m from channel centre: 6% to 10% increase in draw down level magnitude considering Con-S and Tan-L respectively relative to original layout with 8 knot speed.

However, also here MS-b conditions represent a considerable reduction in drawdown magnitude when compared to baseline conditions. This is evident from the bar charts in Figure 3.11 and also applies to the west side of the channel.

The reason for the increase in draw down magnitude at Line-3 relative to MS-a conditions is related to the implemented salt marsh islands east of the channel, which slightly restrict the draw down wave from spreading east into the lagoon.

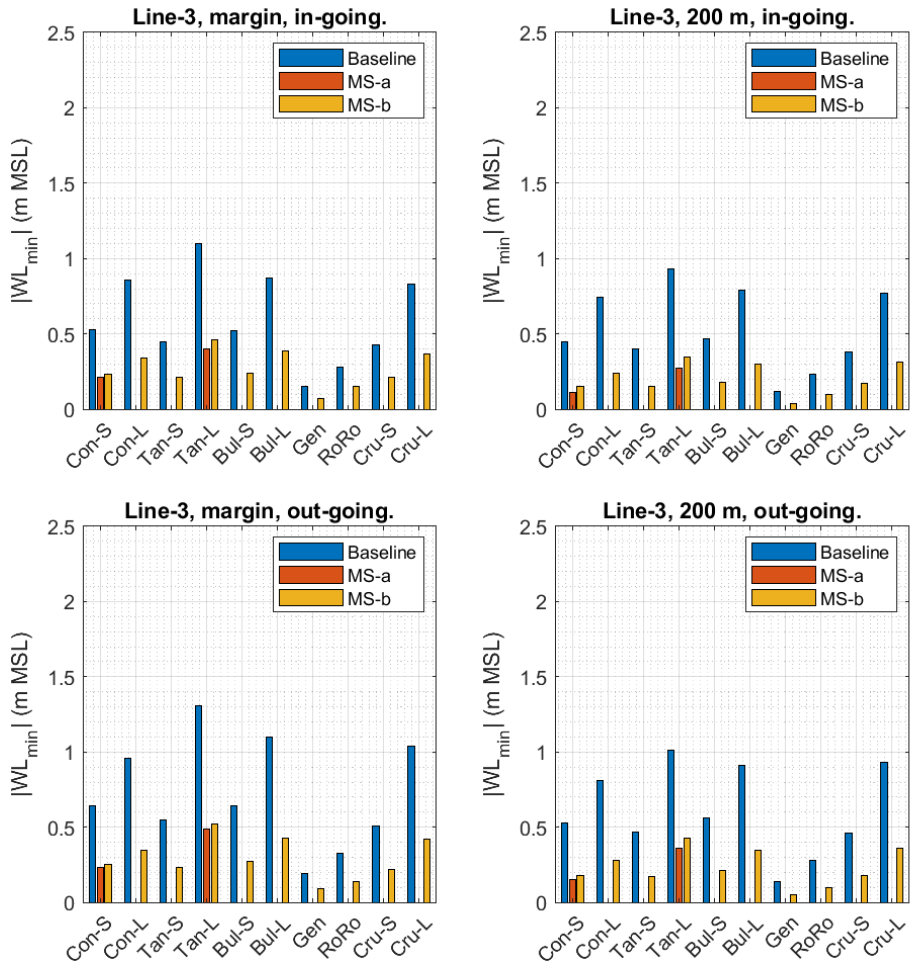

Figure 3.11 Line-3 minimum water level during in- and out-bound passages for MS-b.

Considering the comparisons between MS-a and MS-b draw down levels, it is important to keep in mind, that a wider channel with smoother bends increases navigational safety for both large and small vessels across a wide range of hydrodynamic conditions.

3.3.2 Modelled erosion and bed shear stress

Considering baseline conditions in Table 3-6, the top four vessels in terms of erosion potential for single passages consist solely of the large vessels – listed below starting with the largest erosion potential. Vessels in parentheses account for frequency of occurrence.

1. Tan-L (Tan-L)
2. Cru-L (Con-L)

3. Bul-L (Con-S)
4. Con-L (Bul-L)

The top four vessels account for ~85/75% of the baseline erosion when looking at single passages/over 1 year respectively. This clearly illustrates that the vessel size has significant influence on the magnitude of erosion along the tidal flats of the MMC.

Table 3-6 Eroded volume in polygon considering MS-b.

Relative distribution indicated for single passage (in- + out-bound) and across full year applying the number of occurrences from Table 3-2. Change calculated as scenario relative to baseline. Bottom row contains the total volume magnitude of each column.

	Single Passage			Accumulated 1 year		
	Baseline (%)	MS-b (%)	Change (%)	Baseline (%)	MS-b (%)	Change (%)
Con. S	4	<1	-99	16	3	-89
Con. L	16	5	-97	20	29	-28
Tan. S	2	<1	-98	7	1	-89
Tan. L	26	52	-78	24	35-	-28
Bul. S	6	1	-98	12	3	-89
Bul. L	21	21	-89	15	21	-32
Gen.	<1	<1	-	<1	<1	-
Ro-Ro	1	<1-	-82	<1	<1	-65
Cru. S	2	<1	-98	<1	<1	-89
Cru. L	22	19	-90	5	7	-34
Total (m^3)	~400	~44	~ -275	~51,800	~25,700	~ -26,200

With the new speed limit and the re-designed channel, the modelled total eroded volume inside the polygon has decreased by about 50%. Based on the MS-a results in Section 3.2, the large decrease in erosion volume is mainly related to the decrease in navigation speed.

In Figure 3.12 maps of the modelled erosion level calculated as described in (DHI A/S 2021, [1]) are provided. To account for vessels still having to navigate at 10 knots during some conditions (about 5% of the time), erosion from pure MS-b conditions have been scaled by a factor 0.95 and the original 10 knot results have been superimposed onto the new layout and scaled by a factor 0.05.

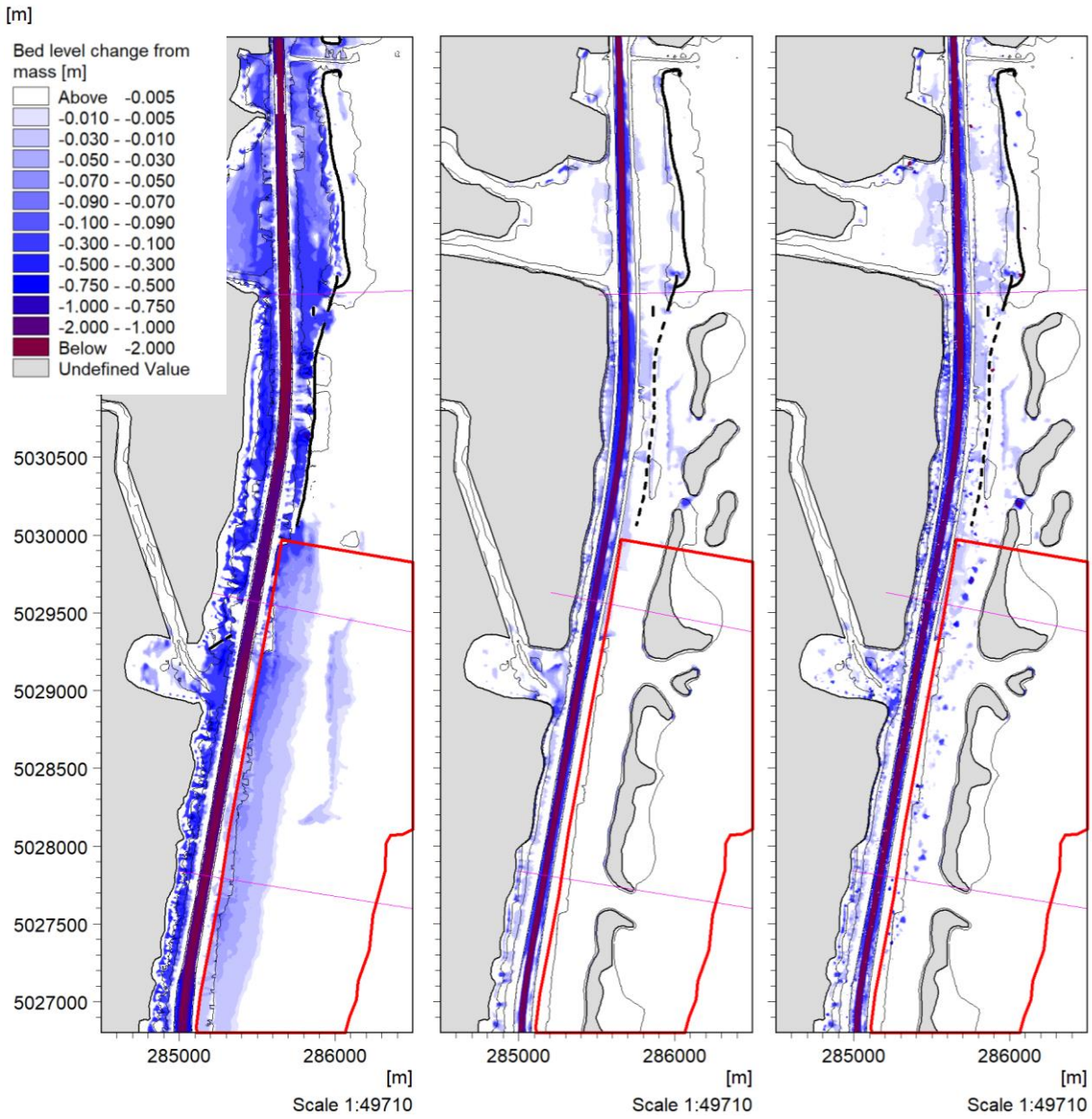

Figure 3.12 Accumulated erosion from modelled vessel traffic, MS-b.

(Left) Existing channel and 10 knots. (Centre) New channel design and 8 knots. (Right) New channel and 8 knots 95% of the time + 10 knot existing channel results scaled to new layout 5% of the time. For the sake of clarity, the color legend only shows the erosion. Red frame indicates the erosion polygon of Figure 3.3.

To add the original 10 knot results, the effect of the new channel layout has been estimated by comparing the erosion from MS-a conditions to that of MS-b conditions:

$$\Delta_{layout} = \frac{\Delta z_{MS-b} - \Delta z_{MS-a}}{\Delta z_{MS-a}} \qquad \textit{Eq. 3.1}$$

This effect has then been added to the original 10 knot results before adding to the pure MS-b results:

$$\Delta z_{8-10\ knots} = \Delta z_{MS-b} \cdot 0.95 + \left(\Delta z_{10\ knots} + \Delta z_{10\ knots} \cdot \Delta_{layout}\right) \cdot 0.05 \qquad \textit{Eq. 3.2}$$

The effect of the layout (Δ_{layout}) has been calculated separately for in- and out-bound passages of Con-S and Tan-L. The effect established for Con-S has then been applied to the smaller vessels (Con-S, Tan-S, Bul-S, Cru-S, Gen. and RoRo) during in- and out-bound passages respectively. Similarly, the effect established for Tan-L has been applied to the larger vessels (Con-L, Tan-L, Bul-L and Cru-L).

From Figure 3.12 it is clear, that MS-b conditions efficiently reduce the erosion of the eastern tidal flats in the area of the erosion polygon. Also, there do not seem to be significant issues with scouring of the channels between the established salt marsh islands in this area.

The erosion (in the area of the erosion polygon) is now mainly seen in the close vicinity to the slopes towards the channel – generally above the -3 m MSL contour. Also, along the shallow slopes on the west side of the established salt marsh islands erosion in the order of a couple of centimetres per year is visible. Hence, these slopes should be expected to become smoother with time. But at considerably shorter time scales than previously – assuming that the vessel traffic remains similar. From Figure 3.13 and Table 3-7 it is clear that the larger vessels are the main cause for the annual erosion along the channel. Table 3-7 contains the ratio between:

- the breadth of the model vessel and 80 m, which is the approximate average width of the redesigned channel cross section with ~12 m depth at extraction Line-1, Line-2 and Line-3.
- the draft of the model vessel and 12 m – the maximum depth of the channel.

It is seen that the annual erosion is linked to high values of these ratios. Another point worth noticing is that the large cruise vessel is responsible for about 7% of the annual erosion volume in the polygon even though the occurrence frequency is considerably lower than for instance Bul-S, see Table 3-2. The reason for this is that the large cruise vessel represents the largest modelled vessel in terms of length and width – its width is comparable to that of the modelled large tanker vessel (its draft however is smaller by about 20%).

Table 3-7 Overview of annual MS-b erosion volume in erosion polygon compared to vessel geometry.

	MS-b (%)	Width ratio Breadth / 80 m (-)	Height ratio Draft / 12m (-)	Width ratio x draft ratio (-)
Con. S	3	0.35	0.75	0.26
Con. L	29	0.37	0.84	0.31
Tan. S	1	0.29	0.77	0.22
Tan. L	35	0.40	0.88	0.35
Bul. S	3	0.32	0.78	0.25
Bul. L	21	0.36	0.88	0.31
Gen.	<1	0.22	0.63	0.14
Ro-Ro	<1	0.33	0.52	0.17
Cru. S	<1	0.34	0.58	0.20
Cru. L	7	0.41	0.69	0.28
Total (m^3)	-25,700	-	-	-

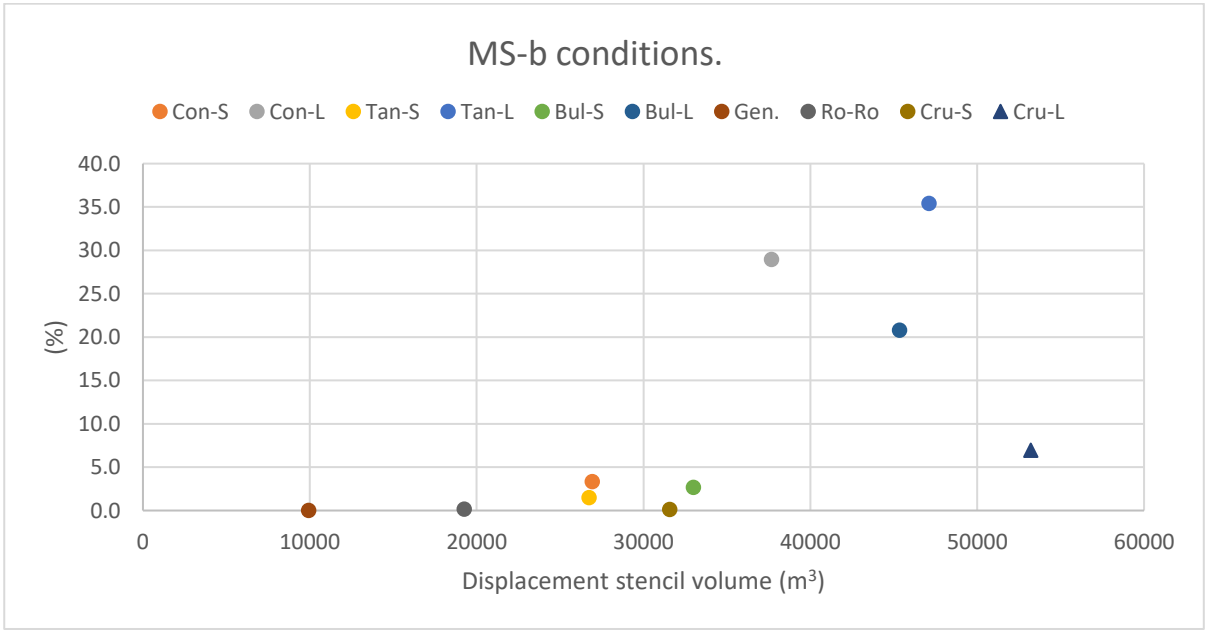

Figure 3.13 Distribution of annually eroded volume percentage in erosion polygon versus vessel displacement stencil volume, MS-b.

North of the erosion polygon, where the original structures have become submerged, the modelled erosion west of the structures above the -3 m MSL contour has decreased from around

0.3 – 0.5 m/year to a couple of centimetres per year. A significant reduction (above 50%) which continues towards the Fusina area. It is also seen that with the submerged structures, the model predicts erosion of a couple of centimetres east of the submerged structures – an area which in the model was previously fully sheltered from the displacement waves by the structures. Erosion in the order of 0.5 m/year is seen in the channel between the cluster of three islands east of the long submerged breakwater. However, the erosion does not appear to spread into the lagoon east of the established salt marsh islands. Therefore, it can be considered a local-scale phenomenon.

Along the west side of the channel, the modelled erosion tends to have decreased to a level comparable to what was originally seen along the east side of the channel between Line-2 and Line-3 i.e., generally below about 0.1 m/year although at the Fusina bend (where the western salt marsh has been restored and the distance to the channel reduced by about 50%) erosion levels similar to existing conditions (order of 0.1 m/year) are seen.

In Figure 3.14 maps of the maximum modelled bed shear stress during the in-bound passage of Tan-L considering Baseline, MS-a and MS-b conditions are shown (note that maps of the maximum modelled suspended sediment concentration are provided in Appendix C). Considering the bed shear stress maps, it is seen that with the new channel design, the modelled bed shear stresses west of the established salt marsh islands (about 1.5 – 3.0 Pa) are higher than during MS-a conditions (about 0.7 – 1.0 Pa).

Compared to baseline conditions however, the bed shear stresses from Tan-L east of the channel are reduced and magnitudes above 0.7 Pa tend to remain west of the salt marsh islands. Especially in the area of the Fusina bend the new layout reduces the bed shear stress magnitudes east of the channel. This effect is mainly linked to the submergence of the breakwaters along the channel combined with the widening of the channel. Along the western side of the channel, the bed shear stress magnitudes remain similar to existing baseline conditions. In this area the third party restoration of the salt marshes is present. This restoration has moved the western shore closer to the channel providing a more restrictive channel in this area and therefore the bed MS-b bed shear stress magnitudes remain large in this area. South of the Fusina bend towards the San Leonardo bend bed shear stress magnitudes about 1.5 – 3.0 Pa are seen east of the channel on to the salt marsh islands i.e., bed shear stresses above 0.7 Pa (the typical erosion threshold of the lagoon) cover a larger distance than during MS-a conditions. In this area the salt marsh islands restrict the spreading of the

displacement wave causing a somewhat stronger but also somewhat more localized impact compared to MS-a conditions.

In the model the salt marsh islands are regarded as dry land when above 0.8 m MSL i.e., they have been excluded from the computational grid. Given the magnitude of the modelled bed shear stresses in Figure 3.14, the slopes of the islands are at risk of erosion – especially during the passage of large vessels with deep drafts, but also smaller vessels can impact the slopes of the salt marsh islands with bed shear stresses above 0.7-1.5 Pa, see Figure 3.15 showing the modelled maximum bed shear stress during the in-bound passage of Con-S. Hence considering longer time scales (about 5 to 10 years) the slopes of these islands (and along the slopes of the reclaimed western salt marshes) will likely need erosion protection or maintenance.

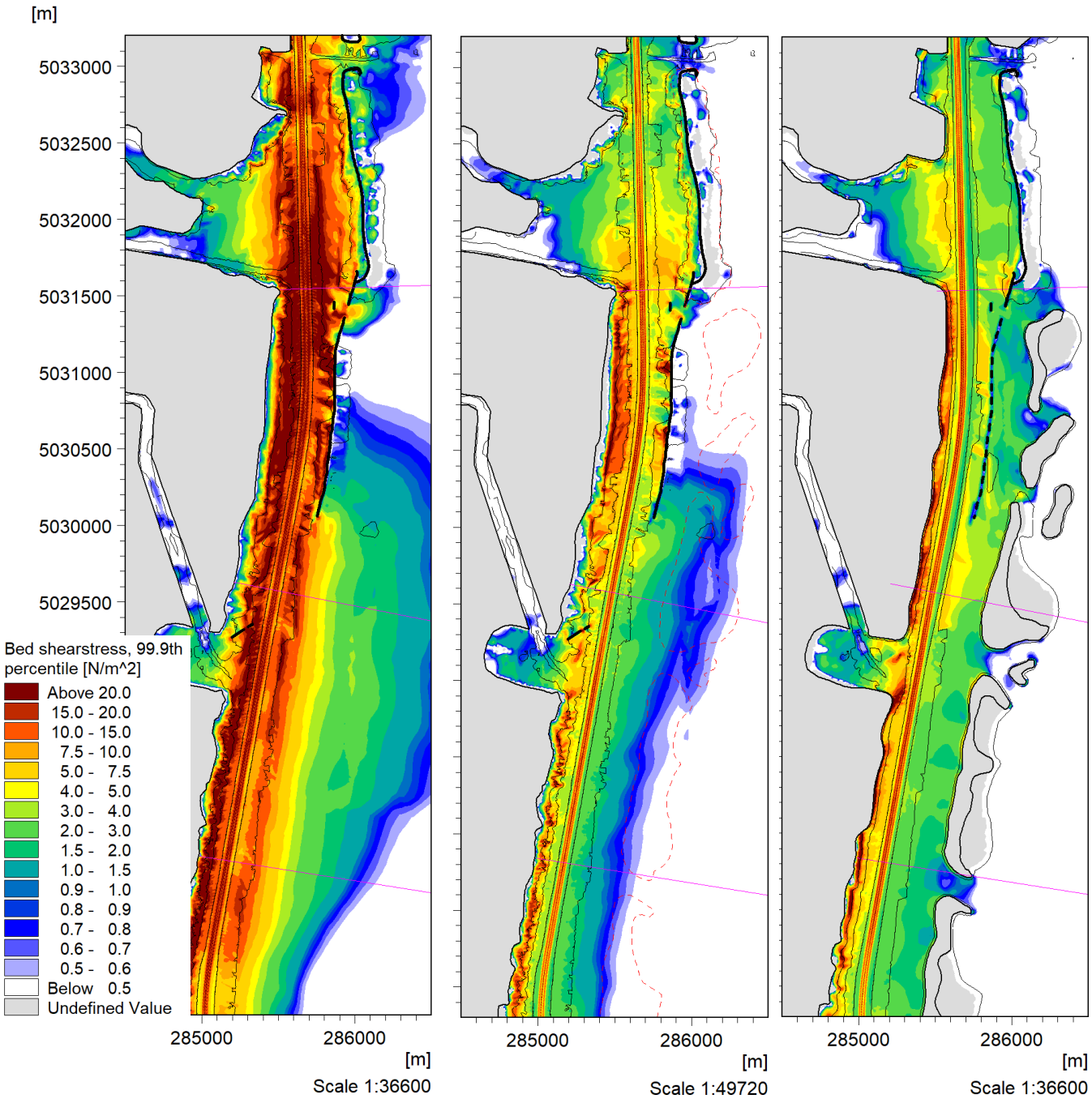

Figure 3.14 *Map of maximum bed shear stress during in-bound passage of Tan-L, MS-b.*

(Left) Existing channel, 10 knots. (Centre) Existing channel, 8 knots. (Right) New channel and 8 knots. Extraction lines marked by pink lines, structures by thick black lines and -10, -3 and -1 m MSL contours by thin black lines.

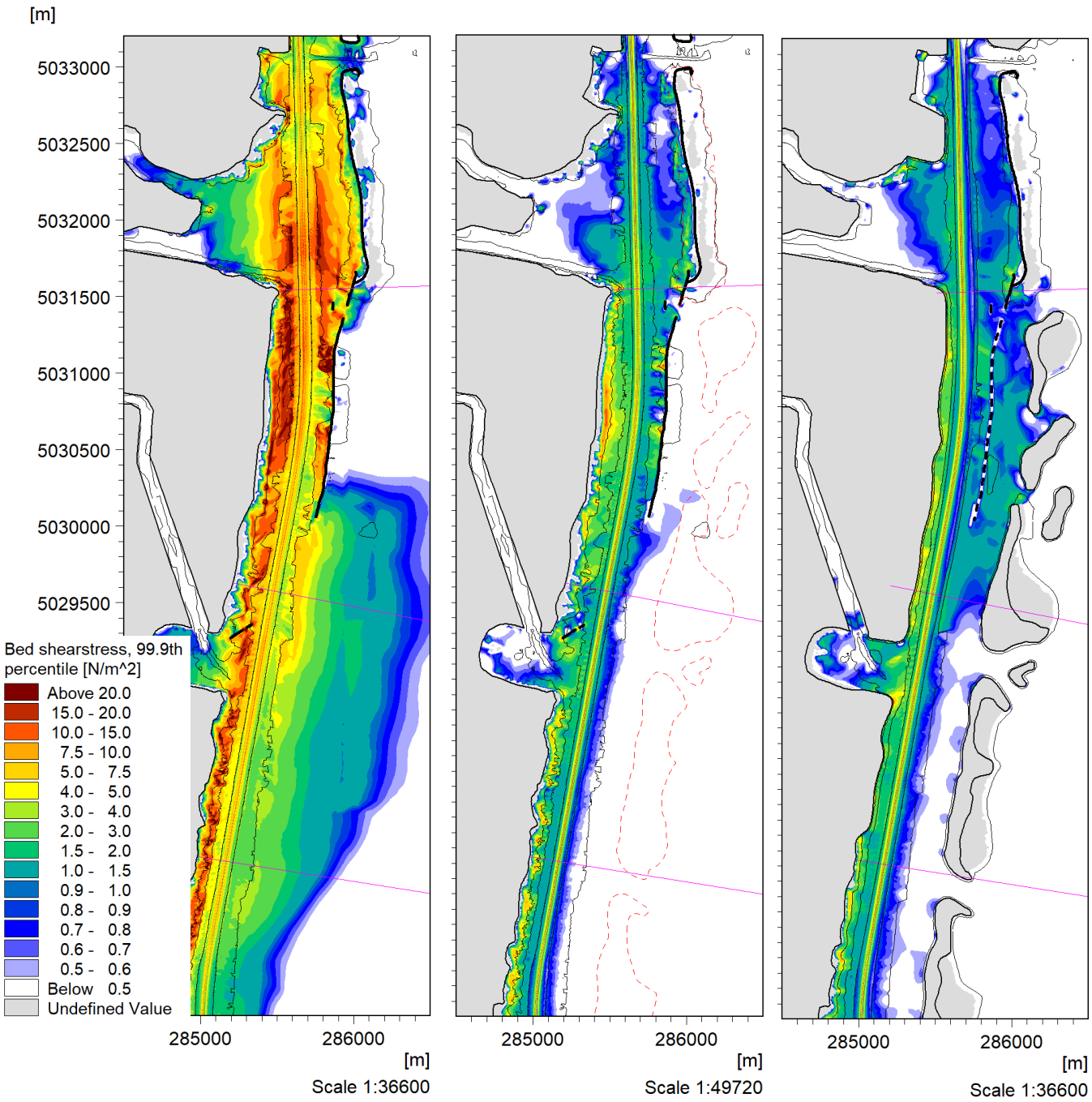

Figure 3.15 *Map of maximum bed shear stress during in-bound passage of Con-S, MS-b.*

(Left) Existing channel, 10 knots. (Centre) Existing channel, 8 knots. (Right) New channel and 8 knots. Extraction lines marked by pink lines, structures by thick black lines and -10, -3 and -1 m MSL contours by thin black lines.

4 CONCLUSIONS

The present report investigates the effect of two mitigative measures addressing the erosion of the tidal flats along the eastern tidal flats of the Malamocco Marghera Channel (MMC) in the lagoon of Venice. The report continues the work provided in (DHI A/S 2022, [1]), which detailed the setup of the used hydrodynamic model for vessel generated displacement waves and sediment transport.

The two mitigation scenarios (MS) investigated here are:

- MS-a: Existing channel with reduction of vessel speed between the San Leonardo bend and Fusina from 10 to 8 knots.
    - Two modelled vessels: Small container vessel (Con-S) and large tanker vessel (Tan-L).
- MS-b: Re-designed channel with reduction of vessel speed between the San Leonardo bend and Fusina from 10 to 8 knots.
    - All vessels from the vessel production matrix (10 vessels).

The re-designed channel layout considers:

- Local widening of the channel in some areas along with smoothing of the channel bend at Fusina.
- Submergence of some breakwaters located along the channel.
- Implementation of salt marsh islands about 400 m from the centre line of the channel starting from the Fusina bend and south on to the San Leonardo bend.

Additionally, restored reclamation areas west of the channel have been implemented in the MS-b model layout along with an extension of the Isola delle Tresse. These effects are included in the model not as mitigation measures but because they are part of third-party plans for the lagoon and as such will co-exist along with the above mentioned mitigative measures.

The below table gives an overview of the volume eroded over one year from the tidal flats east of the channel along the stretch from the San Leonardo bend to just south of the Fusina bend (see the red frame in Figure 3.3) considering Con-S and Tan-L.

The table shows that a 20% reduction in navigation speed reduces the erosion by up to ~90% from smaller vessels (represented by Con-S) considering both MS-a and MS-b conditions. For larger vessels (represented by Tan-L) the erosion reduces by about 80% / 45% considering MS-a / MS-b conditions respectively. In total, the modelled erosion from these two vessels reduces by 85% / 60% considering MS-a / MS-b conditions respectively. The difference between the two layouts in terms of erosion reduction is related to the erosion from displacement waves of the large tanker vessel. Larger vessels cause larger and wider draw down waves. Hence displacement waves from larger vessels experience the new borders of the reclamation area west of the channel as a restriction whereas the displacement waves from smaller vessels are less/unaffected affected by them.

	Eroded volume Accumulated 1 year			Change in volume relative to baseline Accumulated 1 year		
	Con-S (m^3)	Tan-L (m^3)	Total (m^3)	Con-S (%)	Tan-L (%)	Total (%)
Baseline	8,151	16,549	24,700	-	-	-
MS-a	810	2,790	3,600	-90.1	-83.1	-85.4
MS-b	771	8,995	9,766	-90.5	-45.6	-60.5

Considering the full production vessel matrix (representing the annual vessel traffic) over 1 year, the reduced vessel speed combined with the new channel layout leads to a reduction of about 50% in erosion volume (in the erosion polygon, see Figure 3.3) relative to baseline conditions whilst also increasing the navigational safety.

	Eroded volume from all 10 vessels Accumulated 1 year	Change in volume relative to baseline Accumulated 1 year
	Total (m^3)	Total (%)
Baseline	51,800	-
MS-b	25,700	-50.4

The focus area is the central part of the lagoon and as such the implemented salt marsh islands quite effectively protect the lagoon area located more than 400 m east of the channel centreline against erosion from vessel generated displacement waves.

The reduction in erosion volume assumes that the vessels navigating the channel remain of similar size as existing conditions. If the portion of vessels with displacement stencils larger than about 35,000 m^3 will increase in the future, the erosion reduction potential will of course decrease as well.

5 BIBLIOGRAPHY

[1] DHI A/S, “Hydrodynamic simulations: Numerical modelling study of the vessel generated erosion along the Malamocco Marghera Channel - Present Configuration,” DHI A/S, 2022.

[2] “Città di Venezia,” [Online]. Available: https://www.comune.venezia.it/it/content/dati-dalle-stazioni-rilevamento.

[3] C. Amos, G. Umgiesser, C. Ferrarin, C. Thompson, R. Whitehouse, T. Sutherland and A. Bergamasco, “The erosion rates of cohesive sediments in Venice lagoon, Italy.,” *Continental Shelf Research,* 2010.

[4] C. Amos, A. Bergamasco, G. Umgiesser, S. Cappucci, D. Cloutier, L. DeNat, M. Flindt, M. Bonardi and S. Cristante, “The stability of tidal flats in Venice lagoon – the results of in-situ measurements using two benthic, annular flumes,” *Journal Marine Systems,* 2004.

[5] F. Shepard, “Nomenclature based on sand-silt-clay ratios.,” *Journal of Sedimentary Research,* vol. 24, pp. 151-158, 1954.

[6] A. Sarretta, S. Pillon, E. Molinaroli, S. Guerzoni and G. Fontolan, “Sediment budget in the Lagoon of Venice.,” *Continental Shelf Research,* vol. 30, pp. 934-949, 2010.

[7] “Autorità di Sistema Portuale del Mare Adriatico Settentrionale,” [Online]. Available: https://www.port.venice.it/it/autorita-portuale-di-venezia.html. [Accessed 2022].

[8] “Provveditorato Interregionale per le Opere Pubbliche per il Veneto, Trentino Alto Adige e Friuli Venezia Giulia - Ex Magistrato alle Acque - Venezia,” [Online]. Available: http://provveditoratovenezia.mit.gov.it/index.html. [Accessed 2022].

[9] “Consiglio Nazionale delle Ricerche,” [Online]. Available: https://www.cnr.it/. [Accessed 2022].

[10] E. Molinaroli, S. Guerzoni, A. Sarretta, M. Masiol and P. M., “Thirty-year changes (1970 to 2000) in bathymetry and sediment texture recorded in the Lagoon of Venice sub-basins, Italy,” *Marine Geology,* vol. 258, pp. 115-125, 2009.

[11] MIKE by DHI A/S, “MIKE 3 Flow Model FM - Hydrodynamic and Transport Module Scientific Documentation,” DHI A/S, Copenhagen, 2022a.

[12] M. Tondello and B. Mattichio, “Campaign of measurements of speed, current and wave motion generated by the transit of merchant vessels in the Malamocco Marghera Channel,” HS Marine srl, Venice, 2022.

[13] D. L. Kriebel and W. N. Seelig, “An empirical model for ship-generated waves,” in *In proceedings of fifth international symposium on ocean wave measurement and analysis - Waves 2005*, Madrid, 2005.

[14] MIKE by DHI A/S, “MIKE 21 & MIKE 3 Flow Model FM - Mud Transport Module Scientific Documentation,” 2022c.

[15] MIKE by DHI A/S, “MIKE 21 Spectral Wave Module Scientific Documentation,” 2022b.

[16] W. R. D. Dally and R. Dalrymple, “Wave height variation across beaches of arbitrary profile,” *Jounal of Geophysical Research,* vol. 90, no. 10, pp. 11917-11927, 1985.

[17] B. Elfrink, D. M. Hanes and B. G. Ruessink, “Parametrization of near bed orbital velocities under irregular breaking waves on a sloping bed.,” *Coastal Engineering,* vol. 53, pp. 915-927, 2006.

[18] M. Guerrini, G. Fontolan and A. Pedroncini, “Meteomarine and hydrogeological characterization of Venice lagoon,” DHI, 2022.

[19] J. Rapaglia, L. R. K. Zaggia, M. Gelinas and H. Bokuniewicz, “Characteristics of ships' depression waves and associated sediment resuspension in the Venice lagoon Italy,” *Journal of Marine Systems,* vol. 85, pp. 45-56, 2011.

[20] G. M. Scarpa, L. Zaggia, G. Manfè, G. Lorenzetti, K. Parnell, T. Soomere, J. Rapaglia and E. Molinaroli, “The effects of ship wakes in the Venice lagoon and implications for the sustainability of shipping in coastal waters,” *Scientific Reports - Nature Research,* vol. 9, 2019.

[21] L. Zaggia, G. Lorenzetti, G. Manfè, G. M. Scarpa, E. Molinaroli, K. Parnell, J. Rapaglia, M. Gionta and T. Soomere, “Fast shoreline erosion induced by ship wakes in a coastal lagoon: Field evidence and remote sensing analysis,” *PLOS One,* 2017.

[22] PIANC, “Guidelines for protecting berthing structures from scour caused by ships,” PIANC Maritime Navigation Commision, Bruxelles, 2015.

[23] J. H. Verheij, “The stability of bottom and banks subjected to the velocities in the propeller,” in *8th Int. Harbour Congress*, Antwerp, 1983.

[24] J. Fredsøe, “Turbulent boundary layers in wave-current motion,” *Journal of Hydrologic Engineering (ASCE),* vol. 110, no. 8, pp. 1103-1120, 1984.

APPENDICES

Appendix A. Tabularized hydrodynamic and sediment transport results for MS-a conditions

This appendix provides tables of minimum water level, associated bed shear stress and depth averaged SSC-level in the extraction points of the three extraction lines considering MS-a conditions. In the first/second sub-section tables for the east/west side of the channel are presented respectively.

The 10-knot case refers to baseline conditions whereas the 8- knot case refers to Mitigation Scenario a (MS-a) conditions i.e., existing channel layout and reduced speed.

A 1 East side of channel

Table A 1. Modelled Line-1 east-side parameters of Con-S at 8 and 10 knots, existing channel.

Line-1, East		Margin	200 m	400 m	600 m	800 m	1000 m	1200 m	1400 m
Con-S10, In	WL_{min} (m)	-1.05	-0.97	-	-	-	-	-	-
	τ (Pa)	11.3	4.1	-	-	-	-	-	-
	SSC (mg/l)	214.1	1019.9	-	-	-	-	-	-
Con-S10, Out	WL_{min} (m)	-0.61	-0.48	-	-	-	-	-	-
	τ (Pa)	4.4	5.7	-	-	-	-	-	-
	SSC (mg/l)	91.4	421.2	-	-	-	-	-	-
Con-S8, In	WL_{min} (m)	-0.35	-0.25	-	-	-	-	-	-
	τ (Pa)	1.9	1	-	-	-	-	-	-
	SSC (mg/l)	21	5.9	-	-	-	-	-	-
Con-S8,Out	WL_{min} (m)	-0.29	-0.19	-	-	-	-	-	-
	τ (Pa)	1.3	1	-	-	-	-	-	-
	SSC (mg/l)	16.5	11	-	-	-	-	-	-

Table A 2. Modelled Line-2 east-side parameters of Con-S at 8 and 10 knots, existing channel.

Line-2, East		Margin	200 m	400 m	600 m	800 m	1000 m	1200 m	1400 m
Con-S10, In	WL_{min} (m)	-0.67	-0.49	-0.28	-0.22	-0.18	-0.14	-0.12	-0.1
	τ (Pa)	3.9	4.4	1.6	1.2	0.9	0.6	0.4	0.2
	SSC (mg/l)	62.6	306	43.4	55.4	31.9	6.5	3.8	4.3
Con-S10, Out	WL_{min} (m)	-1.06	-0.69	-0.33	-0.22	-0.15	-0.12	-0.1	-0.08
	τ (Pa)	8.3	7.1	1.9	1.2	0.7	0.4	0.3	0.2
	SSC (mg/l)	248.2	823.6	99.6	74.2	14.9	8.9	8.9	9
Con-S8, In	WL_{min} (m)	-0.26	-0.11	-0.09	-0.07	-0.04	-0.03	-0.02	-0.02
	τ (Pa)	1	0.3	0.2	0.2	0.1	0	0	0
	SSC (mg/l)	11.7	3.6	1.8	1.5	1.4	1.2	1.6	2
Con-S8, Out	WL_{min} (m)	-0.34	-0.15	-0.09	-0.07	-0.06	-0.06	-0.05	-0.04
	τ (Pa)	1.4	0.5	0.2	0.2	0.1	0.1	0.1	0
	SSC (mg/l)	15.3	7.9	5.7	5.1	4.8	4.3	4.7	5.2

Table A 3. Modelled Line-3 east-side parameters of Con-S at 8 and 10 knots, existing channel.

Line-3, East		Mar-gin	200 m	400 m	600 m	800 m	1000 m	1200 m	1400 m
Con-S10, In	WL_{min} (m)	-0.53	-0.45	-0.34	-0.25	-0.13	-0.08	-0.05	-0.04
	τ (Pa)	2.6	3	1.8	1	0.3	0.1	0.1	0
	SSC (mg/l)	35.3	68	55.9	9.6	5.9	5.7	5.6	5.9
Con-S10, Out	WL_{min} (m)	-0.64	-0.53	-0.36	-0.28	-0.21	-0.16	-0.13	-0.11
	τ (Pa)	3.5	4	2	1.3	0.8	0.5	0.3	0.2
	SSC (mg/l)	62.5	197.9	98.9	24.9	9.2	8	7.9	8
Con-S8, In	WL_{min} (m)	-0.21	-0.11	-0.07	-0.06	-0.05	-0.03	-0.03	-0.02
	τ (Pa)	0.6	0.2	0.1	0.1	0	0	0	0
	SSC (mg/l)	11.3	6.9	4.1	3.4	3.1	3	3	3.3
Con-S8, Out	WL_{min} (m)	-0.23	-0.15	-0.11	-0.08	-0.06	-0.04	-0.04	-0.03
	τ (Pa)	0.8	0.4	0.2	0.1	0.1	0	0	0
	SSC (mg/l)	11.9	7.9	5.3	4.5	4.1	4.1	4.1	4.4

Table A 4. Modelled Line-1 east-side parameters of Tan-L at 8 and 10 knots, existing channel.

Line-1, East		Margin	200 m	400 m	600 m	800 m	1000 m	1200 m	1400 m
Tan-L10, In	WL_{min} (m)	-2.20	-1.28	-	-	-	-	-	-
	τ (Pa)	57.80	1.90	-	-	-	-	-	-
	SSC (mg/l)	612.90	2051.20	-	-	-	-	-	-
Tan-L10, Out	WL_{min} (m)	-1.19	-0.90	-	-	-	-	-	-
	τ (Pa)	16.00	14.30	-	-	-	-	-	-
	SSC (mg/l)	295.20	772.90	-	-	-	-	-	-
Tan-L8, In	WL_{min} (m)	-0.76	-0.62	-	-	-	-	-	-
	τ (Pa)	7.40	3.40	-	-	-	-	-	-
	SSC (mg/l)	141.10	571.20	-	-	-	-	-	-
Tan-L8, Out	WL_{min} (m)	-0.55	-0.50	-	-	-	-	-	-
	τ (Pa)	4.40	5.50	-	-	-	-	-	-
	SSC (mg/l)	162.80	388.10	-	-	-	-	-	-

Table A 5. Modelled Line-2 east-side parameters of Tan-L at 8 and 10 knots, existing channel.

Line-2, East		Margin	200 m	400 m	600 m	800 m	1000 m	1200 m	1400 m
Tan-L10, In	WL_{min} (m)	-1.27	-0.73	-0.39	-0.29	-0.24	-0.20	-0.17	-0.15
	τ (Pa)	12.60	8.70	2.70	1.80	1.40	1.00	0.70	0.50
	SSC (mg/l)	311.80	846.30	308.60	393.70	206.10	66.80	15.10	4.90
Tan-L10, Out	WL_{min} (m)	-1.91	-0.87	-0.44	-0.28	-0.20	-0.16	-0.14	-0.12
	τ (Pa)	21.70	9.40	2.80	1.60	1.00	0.60	0.40	0.30
	SSC (mg/l)	568.20	979.30	438.40	345.10	77.40	22.20	9.40	9.40
Tan-L8, In	WL_{min} (m)	-0.49	-0.31	-0.20	-0.17	-0.11	-0.07	-0.05	-0.04
	τ (Pa)	2.90	1.80	0.90	0.70	0.40	0.20	0.10	0.10
	SSC (mg/l)	79.40	55.50	4.50	7.70	1.50	1.30	1.60	2.10
Tan-L8, Out	WL_{min} (m)	-0.66	-0.44	-0.22	-0.15	-0.12	-0.11	-0.09	-0.07
	τ (Pa)	4.40	3.40	1.00	0.60	0.40	0.30	0.20	0.10
	SSC (mg/l)	173.10	214.40	11.20	8.00	5.00	4.50	4.80	5.20

Table A 6. Modelled Line-3 east-side parameters of Tan-L at 8 and 10 knots, existing channel.

Line-3, East		Margin	200 m	400 m	600 m	800 m	1000 m	1200 m	1400 m
Tan-L10, In	WL_{min} (m)	-1.10	-0.93	-0.51	-0.37	-0.23	-0.13	-0.09	-0.07
	τ (Pa)	10.30	12.40	3.30	1.90	0.90	0.40	0.20	0.10
	SSC (mg/l)	236.20	589.40	496.50	110.80	10.30	5.90	5.80	5.90
Tan-L10, Out	WL_{min} (m)	-1.31	-1.01	-0.55	-0.40	-0.30	-0.23	-0.18	-0.15
	τ (Pa)	13.20	13.10	4.00	2.20	1.30	0.80	0.60	0.40
	SSC (mg/l)	258.50	615.10	562.10	164.40	35.30	9.70	8.30	8.20
Tan-L8, In	WL_{min} (m)	-0.40	-0.27	-0.19	-0.13	-0.09	-0.07	-0.05	-0.04
	τ (Pa)	2.00	1.20	0.60	0.30	0.20	0.10	0.10	0.00
	SSC (mg/l)	32.30	11.60	4.30	3.50	3.10	3.00	3.00	3.30
Tan-L8, Out	WL_{min} (m)	-0.49	-0.36	-0.26	-0.20	-0.14	-0.10	-0.09	-0.07
	τ (Pa)	2.80	2.00	1.10	0.70	0.40	0.20	0.20	0.10
	SSC (mg/l)	43.50	46.00	13.00	4.70	4.20	4.10	4.20	4.40

A 2 West side of channel

Table A 7. Modelled Line-1 west-side parameters of Con-S at 8 and 10 knots, existing channel.

Line-1, West		Margin	75 m	100 m	125 m	150 m
Con-S10, In	WL_{min} (m)	-1.14	-1.26	-1.13	-0.59	-
	τ (Pa)	9.7	16.1	2.3	0.5	-
	SSC (mg/l)	149.8	416.8	1415.1	345.3	-
Con-S10, Out	WL_{min} (m)	-0.73	-0.76	-0.7	-0.39	-
	τ (Pa)	5.3	10	11.7	5.2	-
	SSC (mg/l)	85.1	246	1234	1370.4	-
Con-S8, In	WL_{min} (m)	-0.41	-0.4	-0.5	-0.55	-
	τ (Pa)	2.2	2.8	5.7	1.7	-
	SSC (mg/l)	24.4	59.8	684.4	460.1	-
Con-S8, Out	WL_{min} (m)	-0.33	-0.31	-0.32	-0.36	-
	τ (Pa)	1.8	2.5	4.8	1.2	-
	SSC (mg/l)	19.1	42	372.6	408.3	-

Table A 8. Modelled Line-2 west-side parameters of Con-S at 8 and 10 knots, existing channel.

Line-2, West		Margin	75 m	100 m	125 m	150 m
Con-S10, In	WL_{min} (m)	-0.82	-0.79	-0.79	-0.79	-1.03
	τ (Pa)	5.5	6.6	7.7	5.6	4.2
	SSC (mg/l)	142.6	174	485.6	440.9	2819.4
Con-S10, Out	WL_{min} (m)	-1.11	-1.11	-1.09	-0.99	-1.13
	τ (Pa)	7.9	10.5	18.7	14.7	8.2
	SSC (mg/l)	266.6	570	590.8	604.8	2603.2
Con-S8, In	WL_{min} (m)	-0.35	-0.33	-0.29	-0.28	-0.29
	τ (Pa)	1.5	1.6	1.4	0.8	0.5
	SSC (mg/l)	15.1	13.7	12.6	7.6	8.5
Con-S8, Out	WL_{min} (m)	-0.33	-0.31	-0.27	-0.24	-0.24
	τ (Pa)	1.2	1.3	1.5	1.3	1.2
	SSC (mg/l)	13.4	13.5	15.4	13.1	14.4

Table A 9. Modelled Line-3 west-side parameters of Con-S at 8 and 10 knots, existing channel.

Line-3, West		Margin	75 m	100 m	125 m	150 m
Con-S10, In	WL_{min} (m)	-0.72	-0.72	-0.77	-0.78	-0.49
	τ (Pa)	4.6	4.6	8.7	13.5	1.7
	SSC (mg/l)	83.7	83.7	745.9	1768.7	1356
Con-S10, Out	WL_{min} (m)	-0.74	-0.74	-0.86	-0.9	-0.48
	τ (Pa)	4.1	4.1	8.5	20.8	4.3
	SSC (mg/l)	118.4	118.4	686.2	2537.3	1966.8
Con-S8, In	WL_{min} (m)	-0.31	-0.31	-0.3	-0.34	-0.46
	τ (Pa)	1.3	1.3	1.8	0.9	1.4
	SSC (mg/l)	12.5	12.5	39.3	221.1	510.4
Con-S8, Out	WL_{min} (m)	-0.27	-0.27	-0.27	-0.32	-0.43
	τ (Pa)	0.9	0.9	1.3	1.7	0.4
	SSC (mg/l)	11.8	11.8	13.3	172.7	79.3

Table A 10. Modelled Line-1 west-side parameters of Tan-L at 8 and 10 knots, existing channel.

Line-1, West		Margin	75 m	100 m	125 m	150 m
Tan-L10, In	WL_{min} (m)	-2.01	-2.29	-1.13	-0.60	-
	τ (Pa)	35.50	39.70	3.40	0.40	-
	SSC (mg/l)	270.70	1399.70	1327.80	249.30	-
Tan-L10, Out	WL_{min} (m)	-1.30	-1.66	-1.01	-0.45	-
	τ (Pa)	17.20	42.30	32.60	2.50	-
	SSC (mg/l)	200.10	806.10	2213.10	1066.30	-
Tan-L8, In	WL_{min} (m)	-0.94	-1.08	-1.11	-0.61	-
	τ (Pa)	9.70	17.60	14.20	0.30	-
	SSC (mg/l)	134.20	347.20	1573.20	345.80	-
Tan-L8, Out	WL_{min} (m)	-0.65	-0.71	-0.73	-0.45	-
	τ (Pa)	6.00	10.50	10.00	0.90	-
	SSC (mg/l)	119.20	233.70	912.60	2904.70	-

Table A 11. Modelled Line-2 west-side parameters of Tan- L at 8 and 10 knots, existing channel.

Line-2, West		Margin	75 m	100 m	125 m	150 m
Tan-L10, In	WL_{min} (m)	-1.33	-1.31	-1.26	-1.31	-1.64
	τ (Pa)	13.30	16.50	17.50	8.70	2.20
	SSC (mg/l)	362.10	511.10	610.00	885.00	6751.90
Tan-L10, Out	WL_{min} (m)	-1.59	-1.78	-1.45	-1.41	-1.54
	τ (Pa)	13.30	23.40	30.40	20.30	5.20
	SSC (mg/l)	649.80	1002.70	940.10	996.20	4187.40
Tan-L8, In	WL_{min} (m)	-0.61	-0.61	-0.59	-0.61	-0.75
	τ (Pa)	3.60	4.30	4.50	3.10	1.80
	SSC (mg/l)	233.80	275.60	302.10	213.40	1103.40
Tan-L8, Out	WL_{min} (m)	-0.63	-0.63	-0.59	-0.57	-0.64
	τ (Pa)	3.90	4.40	6.30	5.60	4.20
	SSC (mg/l)	219.90	339.70	511.80	447.40	891.50

Table A 12. Modelled Line-3 west-side parameters of Tan- L at 8 and 10 knots, existing channel.

Line-3, West		Margin	75 m	100 m	125 m	150 m
Tan-L10, In	WL_{min} (m)	-1.45	-1.45	-1.84	-0.94	-0.54
	τ (Pa)	16.40	16.40	53.00	21.80	3.87
	SSC (mg/l)	344.50	344.50	2569.00	3539.00	651.60
Tan-L10, Out	WL_{min} (m)	-1.42	-1.42	-1.95	-0.99	-0.47
	τ (Pa)	12.00	12.00	49.70	21.20	5.30
	SSC (mg/l)	349.80	349.80	3743.40	3145.60	1904.60
Tan-L8, In	WL_{min} (m)	-0.59	-0.59	-0.63	-0.82	-0.46
	τ (Pa)	4.00	4.00	4.00	3.10	4.10
	SSC (mg/l)	143.60	143.60	736.30	2360.90	2219.30
Tan-L8, Out	WL_{min} (m)	-0.56	-0.56	-0.60	-0.78	-0.40
	τ (Pa)	3.20	3.20	4.40	7.30	2.60
	SSC (mg/l)	70.80	70.80	404.80	1280.80	470.30

Appendix B. Tabularized hydrodynamic and sediment transport results for MS-b conditions

This appendix provides tables of minimum water level, associated bed shear stress and depth averaged SSC-level in the extraction points of the three extraction lines considering MS-b conditions. In the first/second sub-section tables for the east/west side of the channel are presented respectively.

The 10 knot case refers to baseline conditions whereas the 8 knot case refers to Mitigation Scenario b (MS-b) conditions i.e., updated channel layout and reduced speed.

B 1 East side of channel

Table B 1 Modelled Line-1 east-side parameters for Con-S and Con-L during baseline and MS-b conditions.

Line-1, East		Con-S		Con-L	
		Margin	200 m	Margin	200 m
In, 10 knt	WL_{min} (m)	-1.05	-0.97	-2.09	-1.21
	τ (Pa)	11.3	4.1	52.4	4.1
	SSC (mg/l)	214	1020	539	1615
Out, 10 knt	WL_{min} (m)	-0.61	-0.48	-0.90	-0.67
	τ (Pa)	4.4	5.7	8.9	9.6
	SSC (mg/l)	91	421	217	503
In, 8 knt MS-b	WL_{min} (m)	-0.27	-0.21	-0.37	-0.33
	τ (Pa)	0.7	0.9	1.2	1.9
	SSC (mg/l)	12	5	14	69
Out, 8 knt MS-b	WL_{min} (m)	-0.24	-0.18	-0.33	-0.28
	τ (Pa)	0.6	0.6	1.1	1.2
	SSC (mg/l)	14	10	15	22

Table B 2 Modelled Line-2 east-side parameters for Con-S and Con-L during baseline and MS-b conditions.

Line-2, East		Con-S		Con-L	
		Margin	200 m	Margin	200 m
In, 10 knt	WL_{min} (m)	-0.67	-0.49	-1.05	-0.66
	τ (Pa)	3.9	4.4	8.9	7.3
	SSC (mg/l)	63	306	273	765
Out, 10 knt	WL_{min} (m)	-1.06	-0.69	-1.73	-0.81
	τ (Pa)	8.3	7.1	20.1	8.8
	SSC (mg/l)	248	824	371	843
In, 8 knt MS-b	WL_{min} (m)	-0.32	-0.20	-0.46	-0.34
	τ (Pa)	1.2	0.9	2.3	2.0
	SSC (mg/l)	13	4	25	59
Out, 8 knt MS-b	WL_{min} (m)	-0.38	-0.27	-0.51	-0.39
	τ (Pa)	1.5	1.1	2.6	2.1
	SSC (mg/l)	17	11	32	76

Table B 3 Modelled Line-3 east-side parameters for Con-S and Con-L during baseline and MS-b conditions.

Line-3, East		Con-S		Con-L	
		Margin	200 m	Margin	200 m
In, 10 knt	WL_{min} (m)	-0.53	-0.45	-0.86	-0.74
	τ (Pa)	2.6	3.0	6.5	8.0
	SSC (mg/l)	35	68	193	499
Out, 10 knt	WL_{min} (m)	-0.64	-0.53	-0.96	-0.81
	τ (Pa)	3.5	4.0	7.3	8.9
	SSC (mg/l)	63	198	246	525
In, 8 knt MS-b	WL_{min} (m)	-0.23	-0.15	-0.34	-0.24
	τ (Pa)	0.7	0.4	1.3	0.9
	SSC (mg/l)	11	7	15	8
Out, 8 knt MS-b	WL_{min} (m)	-0.25	-0.18	-0.35	-0.28
	τ (Pa)	0.8	0.6	1.3	1.1
	SSC (mg/l)	12	8	16	13

Table B 4 Modelled Line-1 east-side parameters for Tan-S and Tan-L during baseline and MS-b conditions.

Line-1, East		Tan-S		Tan-L	
		Margin	200 m	Margin	200 m
In, 10 knt	WL_{min} (m)	-0.83	-0.88	-2.20	-1.28
	τ (Pa)	7.1	3.1	57.8	1.9
	SSC (mg/l)	163	907	613	2051
Out, 10 knt	WL_{min} (m)	-0.48	-0.40	-1.19	-0.90
	τ (Pa)	2.7	4.1	16.0	14.3
	SSC (mg/l)	59	268	295	773
In, 8 knt MS-b	WL_{min} (m)	-0.24	-0.20	-0.48	-0.47
	τ (Pa)	0.5	0.8	2.0	3.6
	SSC (mg/l)	12	3	43	388
Out, 8 knt MS-b	WL_{min} (m)	-0.21	-0.16	-0.42	-0.38
	τ (Pa)	0.4	0.5	1.7	2.2
	SSC (mg/l)	14	10	23	96

Table B 5 Modelled Line-2 east-side parameters for Tan-S and Tan-L during baseline and MS-b conditions.

Line-2, East		Tan-S		Tan-L	
		Margin	200 m	Margin	200 m
In, 10 knt	WL_{min} (m)	-0.51	-0.43	-1.27	-0.73
	τ (Pa)	2.4	3.3	12.6	8.7
	SSC (mg/l)	41	180	312	846
Out, 10 knt	WL_{min} (m)	-0.79	-0.65	-1.91	-0.87
	τ (Pa)	4.5	6.2	21.7	9.4
	SSC (mg/l)	95	806	568	979
In, 8 knt MS-b	WL_{min} (m)	-0.27	-0.18	-0.59	-0.47
	τ (Pa)	0.9	0.7	3.6	3.5
	SSC (mg/l)	12	4	65	363
Out, 8 knt MS-b	WL_{min} (m)	-0.32	-0.25	-0.69	-0.54
	τ (Pa)	1.1	0.9	4.4	3.9
	SSC (mg/l)	14	9	105	403

Table B 6 Modelled Line-3 east-side parameters for Tan-S and Tan-L during baseline and MS-b conditions.

Line-3, East		Tan-S		Tan-L	
		Margin	200 m	Margin	200 m
In, 10 knt	WL_{min} (m)	-0.45	-0.40	-1.10	-0.93
	τ (Pa)	1.9	2.2	10.3	12.4
	SSC (mg/l)	21	59	236	589
Out, 10 knt	WL_{min} (m)	-0.55	-0.47	-1.31	-1.01
	τ (Pa)	2.6	3.1	13.2	13.1
	SSC (mg/l)	51	105	259	615
In, 8 knt MS-b	WL_{min} (m)	-0.21	-0.15	-0.46	-0.35
	τ (Pa)	0.6	0.4	2.3	1.9
	SSC (mg/l)	11	7	38	40
Out, 8 knt MS-b	WL_{min} (m)	-0.23	-0.17	-0.52	-0.43
	τ (Pa)	0.7	0.5	2.7	2.5
	SSC (mg/l)	12	8	58	93

Table B 7 Modelled Line-1 east-side parameters for Bul-S and Bul-L during baseline and MS-b conditions.

Line-1, East		Bul-S		Bul-L	
		Margin	200 m	Margin	200 m
In, 10 knt	WL_{min} (m)	-1.00	-1.04	-2.16	-1.24
	τ (Pa)	9.9	4.1	53.3	2.8
	SSC (mg/l)	182	1159	598	1866
Out, 10 knt	WL_{min} (m)	-0.54	-0.47	-0.95	-0.79
	τ (Pa)	3.4	5.5	10.0	11.9
	SSC (mg/l)	85	441	233	568
In, 8 knt MS-b	WL_{min} (m)	-0.26	-0.23	-0.40	-0.38
	τ (Pa)	0.7	1.1	1.4	2.4
	SSC (mg/l)	12	10	16	171
Out, 8 knt MS-b	WL_{min} (m)	-0.24	-0.20	-0.35	-0.32
	τ (Pa)	0.6	0.7	1.2	1.5
	SSC (mg/l)	14	10	16	43

Table B 8 Modelled Line-2 east-side parameters for Bul-S and Bul-L during baseline and MS-b conditions.

Line-2, East		Bul-S		Bul-L	
		Margin	200 m	Margin	200 m
In, 10 knt	WL_{min} (m)	-0.57	-0.48	-1.02	-0.68
	τ (Pa)	2.9	4.0	8.3	7.5
	SSC (mg/l)	52	353	271	792
Out, 10 knt	WL_{min} (m)	-0.92	-0.72	-1.79	-0.85
	τ (Pa)	6.0	7.2	21.8	9.0
	SSC (mg/l)	223	823	508	907
In, 8 knt MS-b	WL_{min} (m)	-0.31	-0.22	-0.48	-0.40
	τ (Pa)	1.1	1.0	2.5	2.5
	SSC (mg/l)	13	6	43	142
Out, 8 knt MS-b	WL_{min} (m)	-0.36	-0.29	-0.57	-0.47
	τ (Pa)	1.4	1.3	3.1	2.7
	SSC (mg/l)	17	16	55	250

Table B 9 Modelled Line-3 east-side parameters for Bul-S and Bul-L during baseline and MS-b conditions.

Line-3, East		Bul-S		Bul-L	
		Margin	200 m	Margin	200 m
In, 10 knt	WL_{min} (m)	-0.52	-0.47	-0.87	-0.79
	τ (Pa)	2.4	3.1	6.4	8.8
	SSC (mg/l)	43	101	218	522
Out, 10 knt	WL_{min} (m)	-0.64	-0.56	-1.10	-0.91
	τ (Pa)	3.4	4.2	9.4	11.1
	SSC (mg/l)	83	269	240	587
In, 8 knt MS-b	WL_{min} (m)	-0.24	-0.18	-0.39	-0.30
	τ (Pa)	0.7	0.6	1.7	1.4
	SSC (mg/l)	11	7	21	20
Out, 8 knt MS-b	WL_{min} (m)	-0.27	-0.21	-0.43	-0.35
	τ (Pa)	0.9	0.7	1.9	1.7
	SSC (mg/l)	12	8	29	39

Table B 10 Modelled Line-1 east-side parameters for Gen. and RoRo during baseline and MS-b conditions.

Line-1, East		Gen.		RoRo	
		Margin	200 m	Margin	200 m
In, 10 knt	WL_{min} (m)	-0.27	-0.23	-0.49	-0.49
	τ (Pa)	0.7	0.7	2.5	1.9
	SSC (mg/l)	6	0	35	129
Out, 10 knt	WL_{min} (m)	-0.20	-0.13	-0.32	-0.25
	τ (Pa)	0.5	0.5	1.2	1.6
	SSC (mg/l)	14	13	16	23
In, 8 knt MS-b	WL_{min} (m)	-0.10	-0.07	-0.16	-0.13
	τ (Pa)	0.1	0.1	0.3	0.4
	SSC (mg/l)	12	3	12	2
Out, 8 knt MS-b	WL_{min} (m)	-0.08	-0.06	-0.15	-0.11
	τ (Pa)	0.1	0.0	0.2	0.2
	SSC (mg/l)	14	9	14	10

Table B 11 Modelled Line-2 east-side parameters for Gen. and RoRo during baseline and MS-b conditions.

Line-2, East		Gen.		RoRo	
		Margin	200 m	Margin	200 m
In, 10 knt	WL_{min} (m)	-0.19	-0.12	-0.33	-0.25
	τ (Pa)	0.4	0.3	1.0	1.2
	SSC (mg/l)	12	6	13	11
Out, 10 knt	WL_{min} (m)	-0.26	-0.21	-0.46	-0.42
	τ (Pa)	0.6	0.8	1.8	2.8
	SSC (mg/l)	14	12	20	103
In, 8 knt MS-b	WL_{min} (m)	-0.12	-0.06	-0.19	-0.12
	τ (Pa)	0.2	0.1	0.4	0.3
	SSC (mg/l)	12	4	12	4
Out, 8 knt MS-b	WL_{min} (m)	-0.13	-0.08	-0.21	-0.16
	τ (Pa)	0.2	0.1	0.5	0.4
	SSC (mg/l)	13	8	13	8

Table B 12 Modelled Line-3 east-side parameters for Gen. and RoRo during baseline and MS-b conditions.

Line-3, East		Gen.		RoRo	
		Margin	200 m	Margin	200 m
In, 10 knt	WL_{min} (m)	-0.15	-0.12	-0.28	-0.23
	τ (Pa)	0.2	0.2	0.8	0.8
	SSC (mg/l)	12	9	12	9
Out, 10 knt	WL_{min} (m)	-0.19	-0.14	-0.33	-0.28
	τ (Pa)	0.3	0.3	1.0	1.1
	SSC (mg/l)	13	11	14	13
In, 8 knt MS-b	WL_{min} (m)	-0.07	-0.04	-0.15	-0.10
	τ (Pa)	0.1	0.0	0.3	0.2
	SSC (mg/l)	11	6	11	6
Out, 8 knt MS-b	WL_{min} (m)	-0.09	-0.05	-0.14	-0.10
	τ (Pa)	0.1	0.1	0.3	0.2
	SSC (mg/l)	12	8	12	8

Table B 13 Modelled Line-1 east-side parameters for Cru-S and Cru-L during baseline and MS-b conditions.

Line-1, East		Cru-S		Cru-L	
		Margin	200 m	Margin	200 m
In, 10 knt	WL_{min} (m)	-0.83	-0.93	-2.16	-1.26
	τ (Pa)	6.5	3.4	51.2	1.7
	SSC (mg/l)	171	975	550	2022
Out, 10 knt	WL_{min} (m)	-0.43	-0.40	-0.77	-0.78
	τ (Pa)	2.1	3.7	6.8	10.8
	SSC (mg/l)	42	274	217	535
In, 8 knt MS-b	WL_{min} (m)	-0.22	-0.21	-0.36	-0.38
	τ (Pa)	0.5	0.8	1.2	2.0
	SSC (mg/l)	12	3	15	157
Out, 8 knt MS-b	WL_{min} (m)	-0.22	-0.19	-0.36	-0.35
	τ (Pa)	0.4	0.6	1.1	1.3
	SSC (mg/l)	14	10	16	45

Table B 14 Modelled Line-2 east-side parameters for Cru-S and Cru-L during baseline and MS-b conditions.

Line-2, East		Cru-S		Cru-L	
		Margin	200 m	Margin	200 m
In, 10 knt	WL_{min} (m)	-0.46	-0.40	-0.89	-0.68
	τ (Pa)	1.9	2.7	6.2	7.1
	SSC (mg/l)	22	154	275	790
Out, 10 knt	WL_{min} (m)	-0.72	-0.64	-1.49	-0.87
	τ (Pa)	3.8	5.9	14.7	9.4
	SSC (mg/l)	78	795	415	948
In, 8 knt MS-b	WL_{min} (m)	-0.27	-0.20	-0.45	-0.39
	τ (Pa)	0.8	0.7	2.0	2.2
	SSC (mg/l)	12	4	30	124
Out, 8 knt MS-b	WL_{min} (m)	-0.29	-0.26	-0.49	-0.46
	τ (Pa)	0.9	0.9	2.3	2.4
	SSC (mg/l)	13	9	39	202

Table B 15 Modelled Line-3 east-side parameters for Cru-S and Cru-L during baseline and MS-b conditions.

Line-3, East		Cru-S		Cru-L	
		Margin	200 m	Margin	200 m
In, 10 knt	WL_{min} (m)	-0.43	-0.38	-0.83	-0.77
	τ (Pa)	1.7	2.0	5.8	8.0
	SSC (mg/l)	20	57	217	544
Out, 10 knt	WL_{min} (m)	-0.51	-0.46	-1.04	-0.93
	τ (Pa)	2.2	2.8	8.2	10.9
	SSC (mg/l)	44	109	237	589
In, 8 knt MS-b	WL_{min} (m)	-0.21	-0.17	-0.37	-0.31
	τ (Pa)	0.5	0.4	1.4	1.4
	SSC (mg/l)	11	7	21	18
Out, 8 knt MS-b	WL_{min} (m)	-0.22	-0.18	-0.42	-0.36
	τ (Pa)	0.6	0.5	1.7	1.7
	SSC (mg/l)	12	8	27	45

B 2 West side of channel

Table B 16 Modelled Line-1 west-side parameters for Con-S and Con-L during baseline and MS-b conditions.

Line-1, West		Con-S			Con-L		
		Margin	75 m	100 m	Margin	75 m	100 m
In, 10 knt	WL_{min} (m)	-1.14	-1.26	-1.13	-1.64	-2.06	-1.19
	τ (Pa)	9.7	16.1	2.3	19.7	39.9	2.2
	SSC (mg/l)	150	417	1415	180	1388	1118
Out, 10 knt	WL_{min} (m)	-0.73	-0.76	-0.70	-1.09	-1.29	-0.91
	τ (Pa)	5.3	10.0	11.7	11.6	26.0	30.4
	SSC (mg/l)	85	246	1234	155	461	1361
In, 8 knt MS-b	WL_{min} (m)	-0.34	-0.31	-0.31	-0.47	-0.44	-0.46
	τ (Pa)	1.8	1.7	2.7	3.5	3.4	5.6
	SSC (mg/l)	15	18	136	43	89	369
Out, 8 knt MS-b	WL_{min} (m)	-0.37	-0.36	-0.40	-0.51	-0.51	-0.59
	τ (Pa)	1.8	1.6	2.2	3.1	2.7	4.0
	SSC (mg/l)	21	21	197	49	115	577

Table B 17 Modelled Line-2 west-side parameters for Con-S and Con-L during baseline and MS-b conditions.

Line-2, West		Con-S			Con-L		
		Margin	75 m	100 m	Margin	75 m	100 m
In, 10 knt	WL_{min} (m)	-0.82	-0.79	-0.79	-1.14	-1.15	-1.12
	τ (Pa)	5.5	6.6	7.7	10.0	13.0	15.3
	SSC (mg/l)	143	174	486	305	427	575
Out, 10 knt	WL_{min} (m)	-1.11	-1.11	-1.09	-1.61	-1.74	-1.31
	τ (Pa)	7.9	10.5	18.7	16.1	25.0	26.7
	SSC (mg/l)	267	570	591	447	965	727
In, 8 knt MS-b	WL_{min} (m)	-0.46	-0.46	-0.52	-0.60	-0.61	-0.70
	τ (Pa)	2.5	2.7	3.5	4.0	4.4	4.7
	SSC (mg/l)	32	40	195	92	209	776
Out, 8 knt MS-b	WL_{min} (m)	-0.42	-0.43	-0.48	-0.65	-0.66	-0.75
	τ (Pa)	2.1	2.3	3.4	4.4	5.0	7.4
	SSC (mg/l)	22	31	144	91	170	718

Table B 18 Modelled Line-3 west-side parameters parameters for Con-S and Con-L during baseline and MS-b conditions.

Line-3, West		Con-S			Con-L		
		Margin	75 m	100 m	Margin	75 m	100 m
In, 10 knt	WL_{min} (m)	-0.72	-0.72	-0.77	-1.12	-1.12	-1.42
	τ (Pa)	4.6	4.6	8.7	10.2	10.2	30.0
	SSC (mg/l)	84	84	746	254	254	1782
Out, 10 knt	WL_{min} (m)	-0.74	-0.74	-0.86	-1.28	-1.28	-1.70
	τ (Pa)	4.1	4.1	8.5	11.5	11.5	33.5
	SSC (mg/l)	118	118	686	236	236	2667
In, 8 knt MS-b	WL_{min} (m)	-0.34	-0.34	-0.33	-0.46	-0.46	-0.45
	τ (Pa)	1.5	1.5	1.6	2.5	2.5	2.8
	SSC (mg/l)	14	14	19	44	44	70
Out, 8 knt MS-b	WL_{min} (m)	-0.30	-0.30	-0.28	-0.44	-0.44	-0.43
	τ (Pa)	1.0	1.0	1.1	2.1	2.1	2.4
	SSC (mg/l)	12	12	11	31	31	49

Table B 19 Modelled Line-1 west-side parameters for Tan-S and Tan-L during baseline and MS-b conditions.

Line-1, West		Tan-S			Tan-L		
		Margin	75 m	100 m	Margin	75 m	100 m
In, 10 knt	WL_{min} (m)	-0.92	-1.03	-1.10	-2.01	-2.29	-1.13
	τ (Pa)	3.6	6.4	11.7	35.5	39.7	3.4
	SSC (mg/l)	61	242	1029	271	1400	1328
Out, 10 knt	WL_{min} (m)	-0.58	-0.60	-0.66	-1.30	-1.66	-1.01
	τ (Pa)	5.3	10.0	11.7	17.2	42.3	32.6
	SSC (mg/l)	85	246	1234	200	806	2213
In, 8 knt MS-b	WL_{min} (m)	-0.28	-0.26	-0.25	-0.77	-0.75	-0.80
	τ (Pa)	1.3	1.2	1.8	8.2	8.4	7.7
	SSC (mg/l)	12	10	106	104	216	452
Out, 8 knt MS-b	WL_{min} (m)	-0.33	-0.33	-0.37	-0.75	-0.77	-0.92
	τ (Pa)	1.3	1.2	1.8	5.7	5.0	3.1
	SSC (mg/l)	18	22	195	126	269	705

Table B 20 Modelled Line-2 west-side parameters for Tan-S and Tan-L during baseline and MS-b conditions.

Line-2, West		Tan-S			Tan-L		
		Margin	75 m	100 m	Margin	75 m	100 m
In, 10 knt	WL_{min} (m)	-0.60	-0.61	-0.62	-1.33	-1.31	-1.26
	τ (Pa)	3.1	3.9	4.5	13.3	16.5	17.5
	SSC (mg/l)	87	118	231	362	511	610
Out, 10 knt	WL_{min} (m)	-0.80	-0.81	-0.80	-1.59	-1.78	-1.45
	τ (Pa)	4.4	5.5	9.7	13.3	23.4	30.4
	SSC (mg/l)	176	356	531	650	1003	940
In, 8 knt MS-b	WL_{min} (m)	-0.38	-0.39	-0.45	-0.96	-1.00	-1.17
	τ (Pa)	1.7	1.9	2.7	8.1	9.2	9.0
	SSC (mg/l)	20	33	125	429	448	1056
Out, 8 knt MS-b	WL_{min} (m)	-0.35	-0.36	-0.39	-0.87	-0.89	-1.09
	τ (Pa)	1.5	1.7	2.3	7.2	8.2	10.7
	SSC (mg/l)	16	21	80	382	463	1138

Table B 21 Modelled Line-3 west-side parameters for Tan-S and Tan-L during baseline and MS-b conditions.

Line-3, West		Tan-S			Tan-L		
		Margin	75 m	100 m	Margin	75 m	100 m
In, 10 knt	WL_{min} (m)	-0.61	-0.61	-0.65	-1.45	-1.45	-1.84
	τ (Pa)	3.3	3.3	5.1	16.4	16.4	53.0
	SSC (mg/l)	64	64	755	345	345	2569
Out, 10 knt	WL_{min} (m)	-0.63	-0.63	-0.72	-1.42	-1.42	-1.95
	τ (Pa)	3.1	3.1	5.9	12.0	12.0	49.7
	SSC (mg/l)	50	50	593	350	350	3743
In, 8 knt MS-b	WL_{min} (m)	-0.30	-0.30	-0.30	-0.69	-0.69	-0.71
	τ (Pa)	1.1	1.1	1.3	4.9	4.9	6.1
	SSC (mg/l)	12	12	13	219	219	335
Out, 8 knt MS-b	WL_{min} (m)	-0.27	-0.27	-0.26	-0.64	-0.64	-0.65
	τ (Pa)	0.8	0.8	1.0	4.1	4.1	4.9
	SSC (mg/l)	11	11	10	181	181	310

Table B 22 Modelled Line-1 west-side parameters for Bul-S and Bul-L during baseline and MS-b conditions.

Line-1, West		Bul-S			Bul-L		
		Margin	75 m	100 m	Margin	75 m	100 m
In, 10 knt	WL_{min} (m)	-1.15	-1.34	-1.19	-2.37	-2.27	-1.10
	τ (Pa)	10.1	19.7	1.1	42.1	43.0	5.8
	SSC (mg/l)	147	414	1688	311	1571	1068
Out, 10 knt	WL_{min} (m)	-0.62	-0.70	-0.74	-1.15	-1.43	-1.01
	τ (Pa)	4.3	8.6	8.6	13.0	30.8	27.7
	SSC (mg/l)	114	240	1322	167	522	1854
In, 8 knt MS-b	WL_{min} (m)	-0.31	-0.28	-0.27	-0.58	-0.56	-0.59
	τ (Pa)	1.6	1.5	2.2	5.0	5.2	7.7
	SSC (mg/l)	15	15	96	76	188	522
Out, 8 knt MS-b	WL_{min} (m)	-0.36	-0.36	-0.41	-0.61	-0.62	-0.68
	τ (Pa)	1.6	1.5	1.8	3.7	3.5	2.0
	SSC (mg/l)	22	22	205	118	194	587

Table B 23 Modelled Line-2 west-side parameters for Bul-S and Bul-L during baseline and MS-b conditions.

Line-2, West		Bul-S			Bul-L		
		Margin	75 m	100 m	Margin	75 m	100 m
In, 10 knt	WL_{min} (m)	-0.68	-0.70	-0.72	-1.30	-1.39	-1.24
	τ (Pa)	3.5	4.6	5.4	12.6	18.0	15.5
	SSC (mg/l)	178	270	411	333	550	570
Out, 10 knt	WL_{min} (m)	-0.89	-0.93	-0.96	-1.75	-1.88	-1.39
	τ (Pa)	5.6	7.3	13.5	21.0	28.3	28.6
	SSC (mg/l)	442	625	572	655	864	892
In, 8 knt MS-b	WL_{min} (m)	-0.42	-0.44	-0.51	-0.74	-0.76	-0.87
	τ (Pa)	2.1	2.4	3.2	4.9	5.6	6.1
	SSC (mg/l)	31	58	236	294	390	884
Out, 8 knt MS-b	WL_{min} (m)	-0.39	-0.41	-0.45	-0.68	-0.70	-0.83
	τ (Pa)	1.8	2.1	3.1	4.7	5.3	7.1
	SSC (mg/l)	21	33	102	211	401	812

Table B 24 Modelled Line-3 west-side parameters parameters for Bul-S and Bul-L during baseline and MS-b conditions.

Line-3, West		Bul-S			Bul-L		
		Margin	75 m	100 m	Margin	75 m	100 m
In, 10 knt	WL_{min} (m)	-0.70	-0.70	-0.80	-1.36	-1.36	-1.75
	τ (Pa)	4.4	4.4	5.3	14.4	14.4	39.7
	SSC (mg/l)	109	109	920	327	327	2819
Out, 10 knt	WL_{min} (m)	-0.74	-0.74	-0.88	-1.62	-1.62	-1.98
	τ (Pa)	3.9	3.9	6.7	16.7	16.7	49.9
	SSC (mg/l)	113	113	781	354	354	4402
In, 8 knt MS-b	WL_{min} (m)	-0.34	-0.34	-0.35	-0.55	-0.55	-0.57
	τ (Pa)	1.5	1.5	1.7	3.3	3.3	4.0
	SSC (mg/l)	17	17	23	113	113	226
Out, 8 knt MS-b	WL_{min} (m)	-0.32	-0.32	-0.32	-0.54	-0.54	-0.55
	τ (Pa)	1.2	1.2	1.3	3.0	3.0	3.5
	SSC (mg/l)	13	13	18	86	86	179

Table B 25 Modelled Line-1 west-side parameters for Gen. and RoRo during baseline and MS-b conditions.

Line-1, West		Gen.			RoRo		
		Margin	75 m	100 m	Margin	75 m	100 m
In, 10 knt	WL_{min} (m)	-0.30	-0.29	-0.32	-0.54	-0.56	-0.73
	τ (Pa)	0.8	0.9	2.4	2.4	3.5	6.3
	SSC (mg/l)	12	10	197	32	106	1037
Out, 10 knt	WL_{min} (m)	-0.22	-0.20	-0.20	-0.37	-0.36	-0.40
	τ (Pa)	0.6	0.9	2.4	1.5	2.4	5.6
	SSC (mg/l)	14	14	63	16	53	528
In, 8 knt MS-b	WL_{min} (m)	-0.13	-0.12	-0.11	-0.20	-0.18	-0.18
	τ (Pa)	0.3	0.3	0.4	0.7	0.6	1.1
	SSC (mg/l)	10	8	4	10	8	21
Out, 8 knt MS-b	WL_{min} (m)	-0.13	-0.12	-0.12	-0.21	-0.21	-0.22
	τ (Pa)	0.3	0.2	0.3	0.6	0.6	0.8
	SSC (mg/l)	13	12	9	13	12	21

Table B 26 Modelled Line-2 west-side parameters for Gen. and RoRo during baseline and MS-b conditions.

Line-2, West		Gen.			RoRo		
		Margin	75 m	100 m	Margin	75 m	100 m
In, 10 knt	WL_{min} (m)	-0.26	-0.23	-0.21	-0.38	-0.37	-0.36
	τ (Pa)	0.6	0.7	0.7	1.3	1.5	1.6
	SSC (mg/l)	12	11	9	14	14	18
Out, 10 knt	WL_{min} (m)	-0.29	-0.27	-0.24	-0.48	-0.49	-0.47
	τ (Pa)	0.6	0.7	0.9	1.8	2.2	3.3
	SSC (mg/l)	14	13	13	21	32	95
In, 8 knt MS-b	WL_{min} (m)	-0.17	-0.16	-0.17	-0.24	-0.24	-0.25
	τ (Pa)	0.4	0.4	0.6	0.7	0.8	1.1
	SSC (mg/l)	10	8	4	10	8	6
Out, 8 knt MS-b	WL_{min} (m)	-0.15	-0.14	-0.15	-0.24	-0.24	-0.25
	τ (Pa)	0.3	0.3	0.4	0.7	0.8	1.1
	SSC (mg/l)	12	11	9	12	11	10

Table B 27 Modelled Line-3 west-side parameters for Gen. and RoRo during baseline and MS-b conditions.

Line-3, West		Gen.			RoRo		
		Margin	75 m	100 m	Margin	75 m	100 m
In, 10 knt	WL_{min} (m)	-0.22	-0.22	-0.22	-0.35	-0.35	-0.35
	τ (Pa)	0.5	0.5	0.8	1.2	1.2	2.0
	SSC (mg/l)	12	12	10	13	13	65
Out, 10 knt	WL_{min} (m)	-0.21	-0.21	-0.22	-0.40	-0.40	-0.42
	τ (Pa)	0.4	0.4	0.8	1.3	1.3	2.3
	SSC (mg/l)	13	13	10	14	14	79
In, 8 knt MS-b	WL_{min} (m)	-0.12	-0.12	-0.11	-0.19	-0.19	-0.18
	τ (Pa)	0.2	0.2	0.2	0.5	0.5	0.5
	SSC (mg/l)	11	11	9	11	11	9
Out, 8 knt MS-b	WL_{min} (m)	-0.10	-0.10	-0.09	-0.18	-0.18	-0.17
	τ (Pa)	0.1	0.1	0.1	0.4	0.4	0.4
	SSC (mg/l)	11	11	10	11	11	10

Table B 28 Modelled Line-1 west-side parameters for Cru-S and Cru-L during baseline and MS-b conditions.

Line-1, West		Cru-S			Cru-L		
		Margin	75 m	100 m	Margin	75 m	100 m
In, 10 knt	WL_{min} (m)	-0.94	-1.09	-1.13	-2.21	-2.43	-1.21
	τ (Pa)	6.9	13.3	14.8	42.0	52.6	1.7
	SSC (mg/l)	141	362	1627	470	1543	879
Out, 10 knt	WL_{min} (m)	-0.49	-0.52	-0.64	-0.94	-1.15	-1.06
	τ (Pa)	2.6	4.7	6.9	8.4	17.3	12.7
	SSC (mg/l)	39	223	939	159	356	1643
In, 8 knt MS-b	WL_{min} (m)	-0.27	-0.25	-0.25	-0.39	-0.37	-0.39
	τ (Pa)	1.2	1.2	1.9	2.7	2.6	3.2
	SSC (mg/l)	11	10	92	42	114	316
Out, 8 knt MS-b	WL_{min} (m)	-0.29	-0.29	-0.31	-0.50	-0.50	-0.55
	τ (Pa)	1.0	1.0	1.3	2.6	2.4	2.6
	SSC (mg/l)	14	14	107	57	119	421

Table B 29 Modelled Line-2 west-side parameters for Cru-S and Cru-L during baseline and MS-b conditions.

Line-2, West		Cru-S			Cru-L		
		Margin	75 m	100 m	Margin	75 m	100 m
In, 10 knt	WL_{min} (m)	-0.50	-0.51	-0.53	-1.02	-1.02	-1.14
	τ (Pa)	2.0	2.5	2.7	7.1	8.9	10.3
	SSC (mg/l)	42	56	101	308	464	528
Out, 10 knt	WL_{min} (m)	-0.74	-0.75	-0.78	-1.62	-1.75	-1.51
	τ (Pa)	3.8	4.7	8.5	15.1	18.0	28.1
	SSC (mg/l)	178	387	540	588	1475	932
In, 8 knt MS-b	WL_{min} (m)	-0.31	-0.32	-0.35	-0.57	-0.58	-0.64
	τ (Pa)	1.1	1.3	1.7	3.2	3.6	4.1
	SSC (mg/l)	13	14	38	112	174	513
Out, 8 knt MS-b	WL_{min} (m)	-0.32	-0.32	-0.34	-0.51	-0.51	-0.55
	τ (Pa)	1.2	1.3	1.7	2.8	3.0	3.7
	SSC (mg/l)	13	18	28	84	156	336

Table B 30 Modelled Line-3 west-side parameters for Cru-S and Cru-L during baseline and MS-b conditions.

Line-3, West		Cru-S			Cru-L		
		Margin	75 m	100 m	Margin	75 m	100 m
In, 10 knt	WL_{min} (m)	-0.53	-0.53	-0.57	-1.14	-1.14	-1.57
	τ (Pa)	2.5	2.5	3.3	9.5	9.5	18.7
	SSC (mg/l)	43	43	694	311	311	2631
Out, 10 knt	WL_{min} (m)	-0.63	-0.63	-0.72	-1.37	-1.37	-1.76
	τ (Pa)	2.8	2.8	4.6	10.6	10.6	21.4
	SSC (mg/l)	50	50	547	298	298	3749
In, 8 knt MS-b	WL_{min} (m)	-0.27	-0.27	-0.27	-0.48	-0.48	-0.50
	τ (Pa)	0.9	0.9	1.0	2.5	2.5	3.1
	SSC (mg/l)	11	11	10	60	60	126
Out, 8 knt MS-b	WL_{min} (m)	-0.26	-0.26	-0.27	-0.47	-0.47	-0.49
	τ (Pa)	0.8	0.8	0.9	2.2	2.2	2.6
	SSC (mg/l)	11	11	10	40	40	104

Appendix C. Maps of Suspended Sediment Concentration

This appendix provides maps of the maximum modelled (surface and depth averaged) Suspended Sediment Concentration (SSC) during MS-a and MS-b conditions considering the in-bound passage of Con-S and Tan-L.

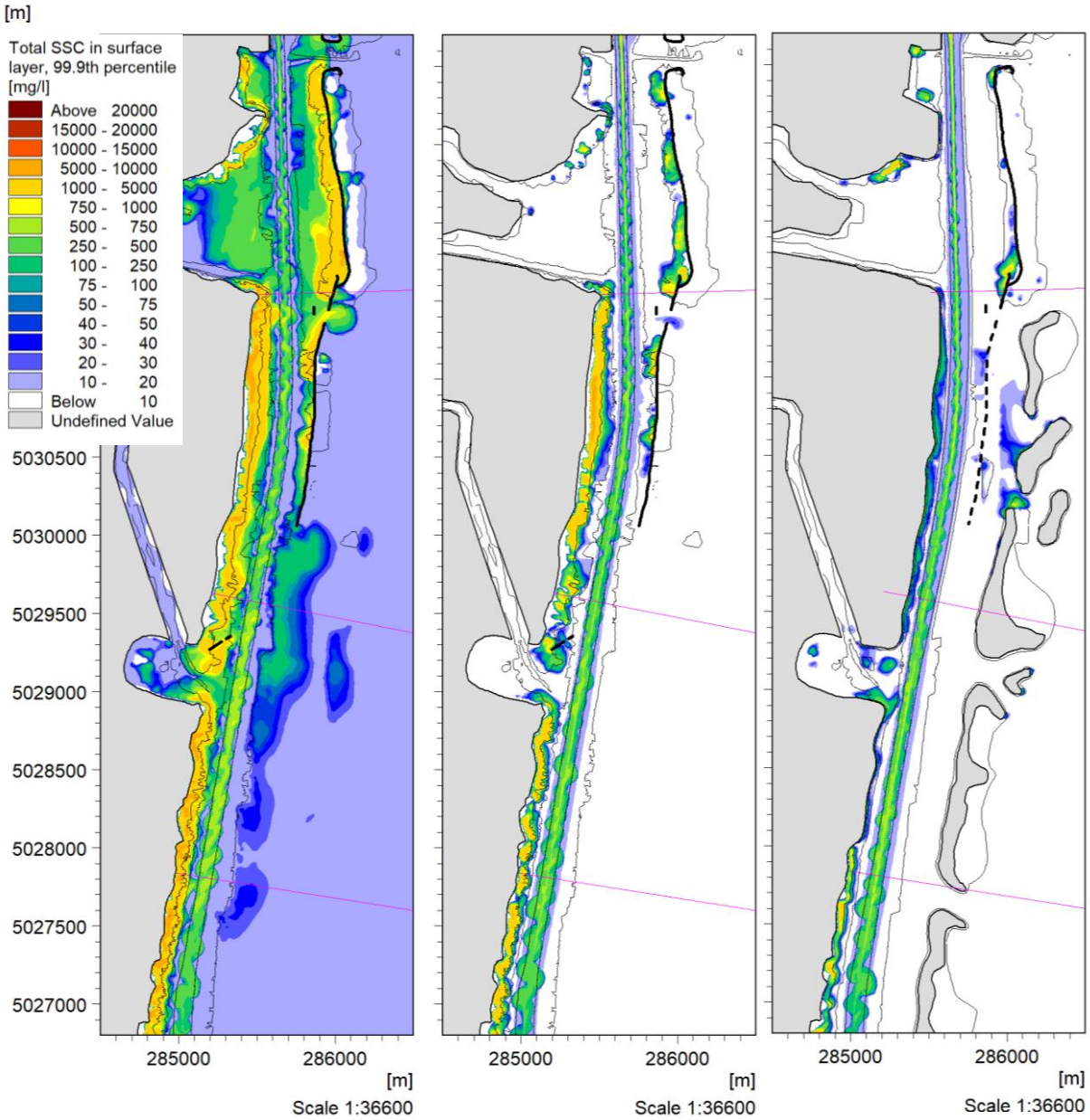

Figure C 1 Maximum SSC in model surface layer during in-bound passage of Con-S. (Left) 10 knots existing layout. (Middle) 8 knots existing layout. (Right) 8 knots updated layout.

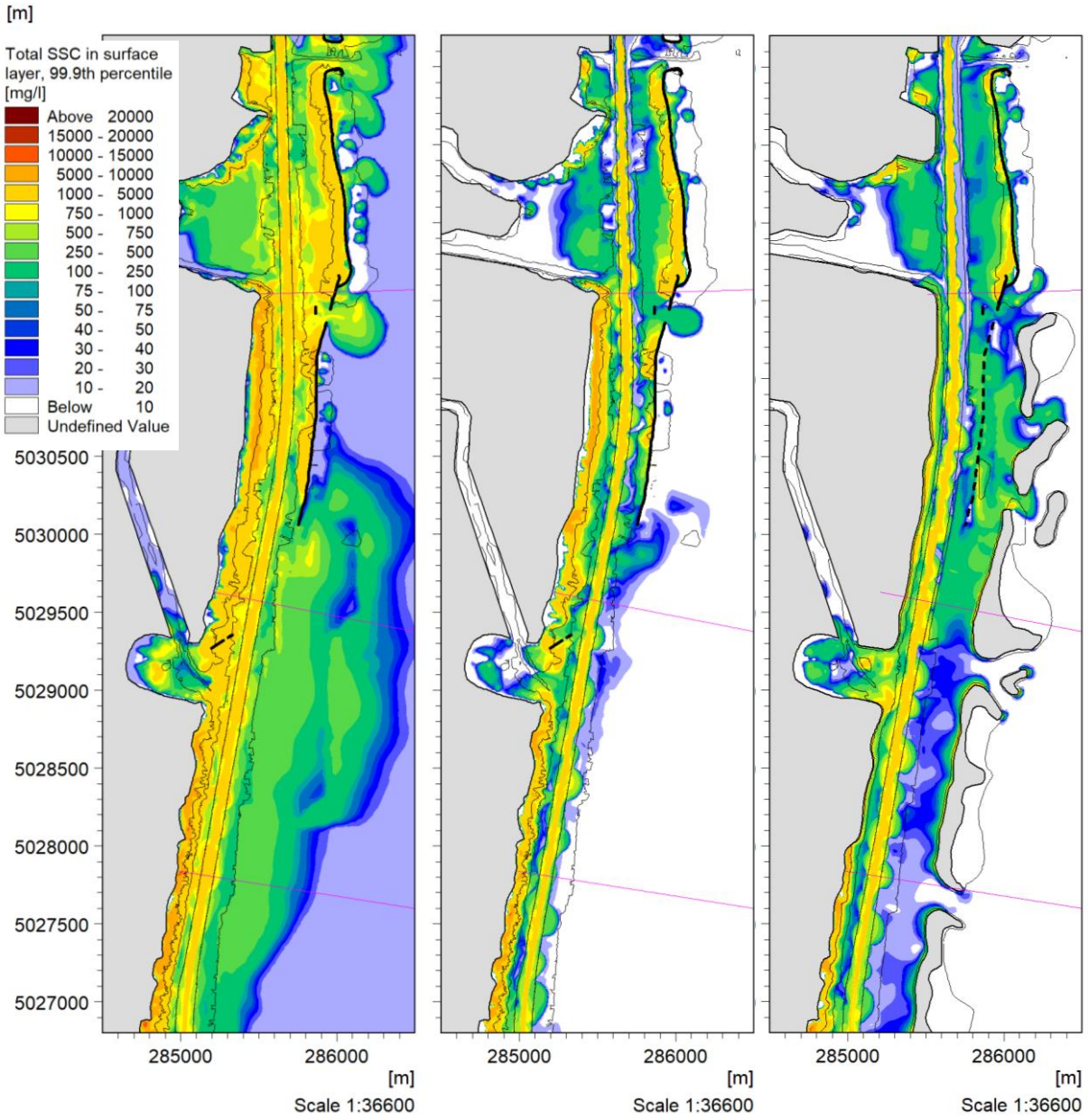

Figure C 2 Maximum SSC in model surface layer during in-bound passage of Tan-L. (Left) 10 knots existing layout. (Middle) 8 knots existing layout. (Right) 8 knots updated layout.

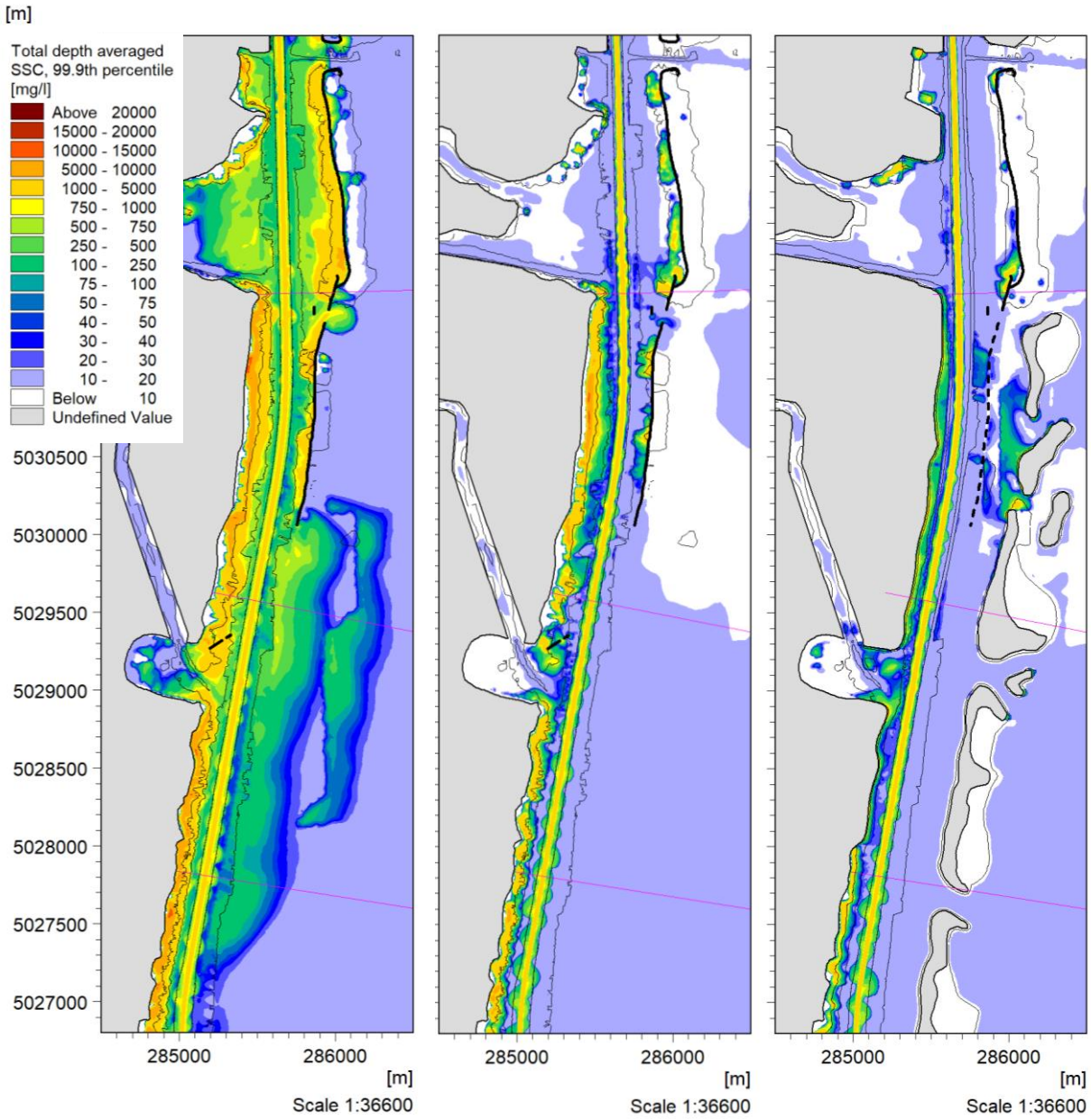

Figure C 3 Maximum depth averaged SSC during in-bound passage of Con-S. (Left) 10 knots existing layout. (Middle) 8 knots existing layout. (Right) 8 knots updated layout.

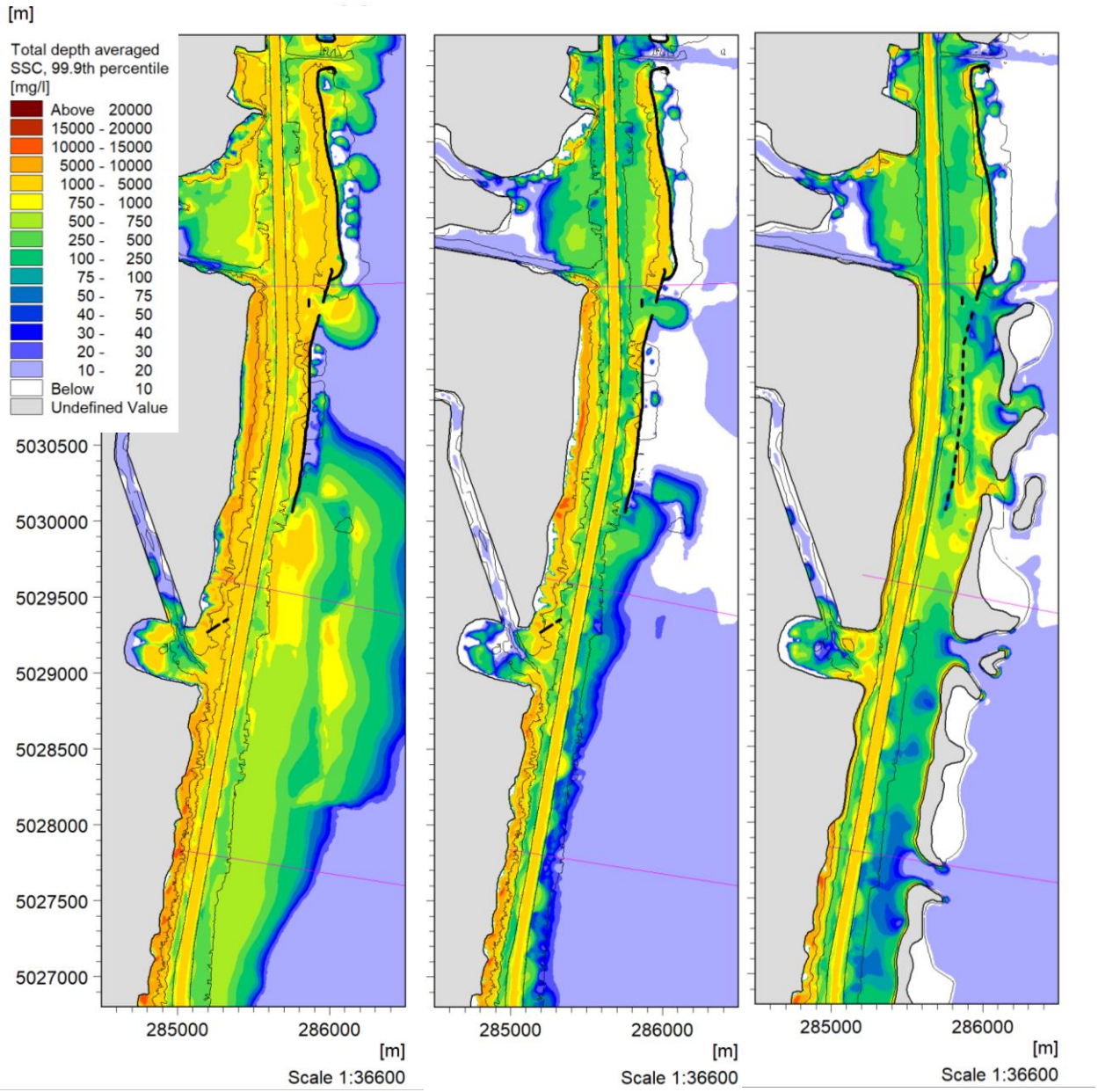

Figure C 4 Maximum depth averaged SSC during in-bound passage of Tan-L. (Left) 10 knots existing layout. (Middle) 8 knots existing layout. (Right) 8 knots updated layout.